AWARD NUMBER: W81XWH-14-1-0184

TITLE: Hyaluronan-Based Therapy for Metastatic Prostate Cancer

PRINCIPAL INVESTIGATOR:Magdalena Swierczewska

CONTRACTING ORGANIZATION: JOHNS HOPKINS UNIVERSITY
BALTIMORE MD 21218-2680

REPORT DATE: September 2016

TYPE OF REPORT: Final

PREPARED FOR: U.S. Army Medical Research and Materiel Command
Fort Detrick, Maryland 21702-5012

REPORT DOCUMENTATION PAGE

Form Approved
OMB No. 0704-0188

1. REPORT DATE	2. REPORT TYPE	3. DATES COVERED
September 2016	Final	25 Jun 2014 - 18 Mar 2016

4. TITLE AND SUBTITLE

Hyaluronan-Based Therapy for Metastatic Prostate Cancer

5a. CONTRACT NUMBER

5b. GRANT NUMBER
W81XWH-14-1-0184

5c. PROGRAM ELEMENT NUMBER

6. AUTHOR(S)

Magdalena Swierczewska

E-Mail: maggieswier@gmail.com

5d. PROJECT NUMBER

5e. TASK NUMBER

5f. WORK UNIT NUMBER

7. PERFORMING ORGANIZATION NAME(S) AND ADDRESS(ES)

JOHNS HOPKINS UNIVERSITY, THE
3400 N CHARLES ST W400 WYMAN PARK BLDG
BALTIMORE MD 21218-2680

8. PERFORMING ORGANIZATION REPORT NUMBER

9. SPONSORING / MONITORING AGENCY NAME(S) AND ADDRESS(ES)

U.S. Army Medical Research and Materiel Command
Fort Detrick, Maryland 21702-5012

10. SPONSOR/MONITOR'S ACRONYM(S)

11. SPONSOR/MONITOR'S REPORT NUMBER(S)

12. DISTRIBUTION / AVAILABILITY STATEMENT

Approved for Public Release; Distribution Unlimited

13. SUPPLEMENTARY NOTES

14. ABSTRACT

In this Prostate Cancer Research Program Postdoctoral Training Award, the research goal is to develop a prostate cancer-targeted nanoplatform for imaging and drug delivery using a hyaluronic acid (HA)-based nanoparticle. The HA-degrading enzyme, hyaluronidase (Hyal), is used as a biomarker for progressive prostate cancer cells. By using nanomedicine, anticancer drugs can localize at the specific tumor site thereby reducing side effects on healthy tissue, which is particularly important when the average age of the patient at the time of diagnosis is 67. The HA-based nanoparticle carries anti-cancer drugs in it center cores, and the drug can be released by enzymatic degradation via HYAL1. Importantly, the system can target CD44+ prostate cancer stem cells through intrinsic HA-CD44 receptor interactions and deliver drugs directly to tumor-initiating cells. The study aims to meet the PCRP Overarching Challenge to develop effective treatments for men with high risk of metastatic prostate cancer. The training goal is to apply the PI's interdisciplinary training in imaging and nanotechnology towards clinical translation of theranostic (therapeutic + diagnostic) agents.

15. SUBJECT TERMS

Hyaluronan, Nanomedicine, Targeted Therapies, Drug Delivery, Theranostics, Hyaluronidase

16. SECURITY CLASSIFICATION OF:			17. LIMITATION OF ABSTRACT	18. NUMBER OF PAGES	19a. NAME OF RESPONSIBLE PERSON
a. REPORT	b. ABSTRACT	c. THIS PAGE			USAMRMC
U	U	U	UU	41	19b. TELEPHONE NUMBER *(include area code)*

Table of Contents

Page

1. INTRODUCTION

In this Prostate Cancer Research Program Postdoctoral Training Award, the research goal is to develop a prostate cancer-targeted nanoplatform for imaging and drug delivery using a hyaluronic acid (HA)-based nanoparticle. The HA-degrading enzyme, hyaluronidase (Hyal), is used as a biomarker for progressive prostate cancer cells. By using nanomedicine, anticancer drugs can localize at the specific tumor site thereby reducing side effects on healthy tissue, which is particularly important when the average age of the patient at the time of diagnosis is 67. The HA-based nanoparticle carries anti-cancer drugs in it center cores, and the drug can be released by enzymatic degradation via HYAL1. Importantly, the system can target CD44+ prostate cancer stem cells through intrinsic HA-CD44 receptor interactions and deliver drugs directly to tumor-initiating cells. The study aims to meet the PCRP Overarching Challenge to develop effective treatments for men with high risk of metastatic prostate cancer. The training goal is to apply the PI's interdisciplinary training in imaging and nanotechnology towards clinical translation of theranostic (therapeutic + diagnostic) agents.

2. KEYWORDS

Hyaluronic Acid, Hyaluronan, Nanomedicine, Nanoparticles, Targeted Therapies, Drug Delivery, Theranostics, Hyaluronidase

3. ACCOMPLISHMENTS

a) Major Goals of the Project

The Research-Specific Tasks of the approved SOW are listed below for Year 1 and 2. The progress of the task are included in the third column by the percentage of completion.

Research-Specific Tasks:	**Months**	**Percent Completed**
Specific Aim 1: To characterize fluorescence activation of dye/quencher labeled HA-based nanoparticles	1-7	
Major Task: Conjugate and measure fluorescence of hydrophobically modified HA nanoparticles with dye-quencher pairs at varying concentrations		
Subtask 1: Conjugate Cy5.5 dye and BHQ3 quencher onto HA backbone along with cholanic acid as the hydrophobic moiety and determine appropriate ratios for effective fluorescence quenching	1-3	100% Sept. 2014
Subtask 2: Test optimized platform in varying concentrations of HYAL1, pH conditions and non-specific enzymes and determine correlation between HYAL1 concentration and fluorescence	3-6	90%
Subtask 3: Characterize fluorescence activation nanoplatform in cancerous and non-cancerous cell lines Cell lines used: Cancerous: LNCaP, DU-145, PC-3; Non-cancerous: PrEC	6	75%
Milestone(s) Achieved: Discovery of a fluorescence activatable HA-based system for detection of overexpressed HYAL1		
Specific Aim 2: Determine cell uptake and toxicity of drug loaded HA-based nanoparticles	**7-14**	
Major Task: Develop docetaxel -loaded and conjugated HA-NPs		
Subtask 1: Conjugate DTX to HA backbone or load into HA nanoformulation	7	100% Oct. 2014

Subtask 2: Treat drug loaded, drug-free HA nanoparticles and drug alone to cancerous and non-cancerous cell lines and measure cell uptake by fluorescence activated cell sorting Cell lines used: Cancerous: LNCaP, DU-145, PC-3; Non-cancerous: PrEC	7-12	100% Feb. 2015
Subtask 3: Treat drug loaded, drug-free HA nanoparticles and drug alone to cancerous and non-cancerous cell lines and measure cell toxicity Cell lines used: Cancerous: LNCaP, DU-145, PC-3; Non-cancerous: PrEC, PZHPV-7	7-14	50%
Milestone(s) Achieved: Identification of lead HA-based nanotherapeutic for prostate cancer cells		
Specific Aim 3: To identify the biodistribution, targeting efficacy and therapeutic potential of lead compound from Aim 1 and 2 in an *in vivo* mouse tumor model	**14-24**	
Major Task: PET and optical labeling/imaging of HA-based theranostic for prostate cancer		
Subtask 1: Label nanoplatform with drug/dye/radiolabel	14-15	50%
Subtask 2: Optimize injection concentration to image fluorescence activation and perform preliminary biodistribution	15-17	100%
Subtask 3: Treat mouse tumor model by intravenous injection and undergo PET/optical imaging at staggering days for 1 week	18	100%
Subtask 4: Measure injected dose/gram and tumor size for 1 month	18-20	0%
Milestone(s) Achieved: Analysis of therapeutic efficacy and imaging capabilities of HA-based nanoplatform for prostate cancer	20-24	

b) Accomplished Under These Goals

The specific objective under these goals was to develop florescence activatable HA-NPs and determine drug delivery by HA-NPs in prostate cancer in vitro and in vivo.

Year 1:

Fluorescence activatable HA-NPs were successfully synthesized by coupling the hydrophobically modified HA with the near infrared (NIR) fluorophore Cy5.5 and the NIR quencher BHQ3 via EDC/NHS chemistry (Figure Appendix 1). An optimized mole ratio between the dye-quencher pair was measured based on fluorescence quenching and recovery values of the HA-NP using a fluorescence spectrophotometer at ex/em: 675 nm/695 nm (Figure 1). A ratio of 2:1 BHQ-3:Cy5.5 was chosen for HA-NPs, because that ratio preserves materials without making a significant effect in the fluorescence quenching (Figure 1A).

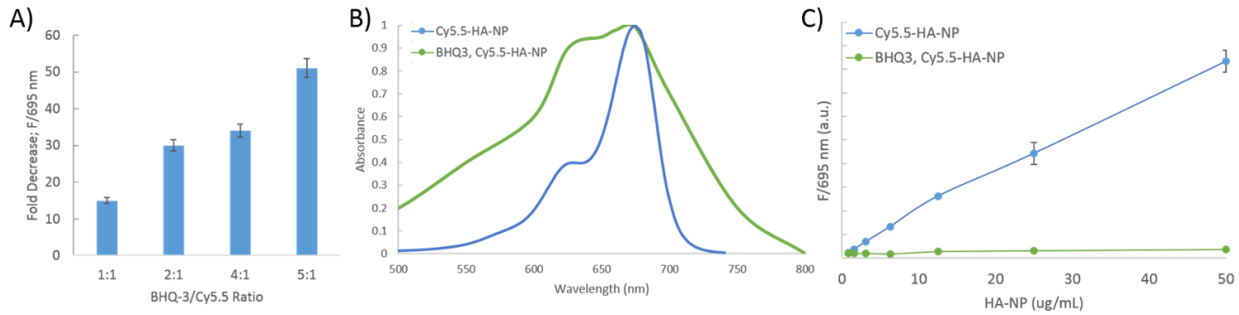

Figure 1: Characterization of HA-NPs conjugated with Cy5.5 and BHQ-3. A) HA-NPs conjugated with numerous ratios of BHQ-3 and Cy5.5 were examined for their ability to quench Cy5.5 fluorescence. Fluorescence fold decrease was measured between BHQ3, Cy5.5-HA-NPs and Cy5.5-HA-NPs normalized to the same concentration of dye. B) Normalized absorbance of Cy5.5-HA-NPs and BHQ-3, Cy5.5-HA-NP (2:1 ratio). C) Fluorescence measurements between Cy5.5-HA-NPs and BHQ3, Cy5.5-HA-NPs compared at various concentrations of HA-NPs.

The significant outcome was an optimized protocol included in Appendix I.A-B to develop NIR fluorescence activatable HA-NPs (**Specific Aim 1, Subtask 1**). Next fluorescence quenching stability of the HA-NPs were monitored at pHs of 3, 7, and 10, and compared with the same concentration of Cy5.5 dye at identical conditions. Fluorescence activation monitored after HYAL concentrations between 0-200 units/mL at pH 4.5 for up to 2 hours indicated that HA-NPs recover fluorescence in a time dependent and enzyme activity dependent manner (Figure 2).

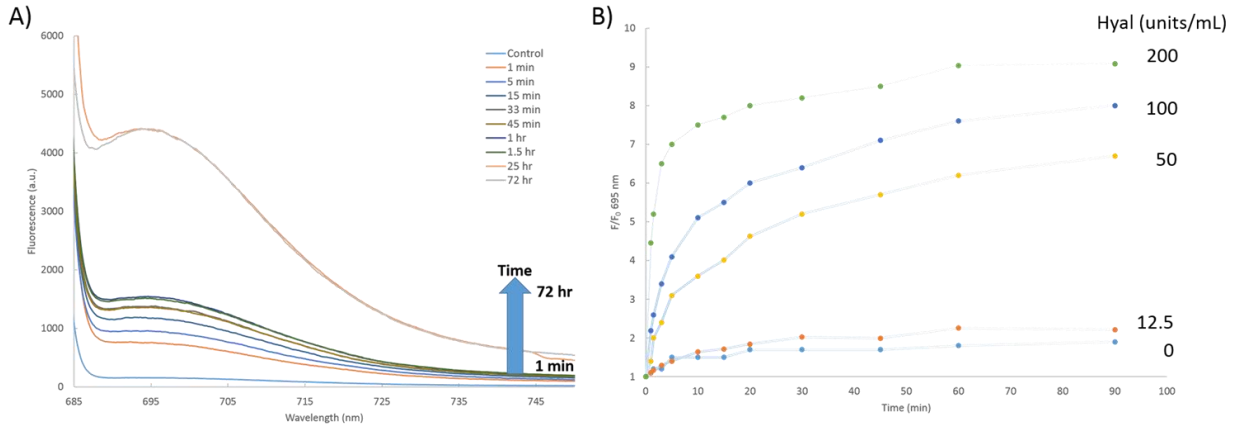

Figure 2: Fluorescence activation of BHQ3-Cy5.5-HA-NPs when treated with hyaluronidase (HYAL) concentration. A) Fluorescence spectra of HA-NPs incubated with 200 units/mL at pH 4.5 from 1 minute to 72 hours and compared with no HYAL treatment (Control). B) Fluorescence fold recovery measurement from initial fluorescent measurement (F/F_0) of HA-NPs over time with different HYAL activities.

However, complete fluorescence to the Cy5.5 concentration control was not recovered, which may be due to the constant concentration of quenchers found in the cuvette. Overall, these results imply that HA-NPs are properly conjugated with dye-quencher pairs and can be stable in physiological conditions. Additionally, HA-NPs can under fluorescence activation with the addition of HYAL enzyme, indicating that they can be used to detect HYAL in vivo and trigger drug release. Additional studies are required to investigate their stability in non-specific enzymes, trypsin and glutathione (**Specific Aim 1, Subtask 2**). To investigate uptake of HA-NPs by prostate cancer cells, CD44 receptor expression levels were first investigated in prostate cancer cell lines (HP LNCAP, DU145, and PC-3) and compared with the expression levels to a positive control, human colon carcinoma cell line HCT116, and a negative control, human embryonic kidney cell line HEK293T,

using western blot analysis. In general, western blot analysis was performed by first lysing cells by sonication, clarifying by centrifugation and resolving by SDS-PAGE. The proteins were then transferred onto nitrocellulose, blocked with albumin and incubated overnight with anti-CD44 and anti-GAPDH primary antibodies. High CD44 expressing prostate cancer cell lines (PC3, DU145) correlate with greater tumorigenic and metastatic properties over prostate cancer cell lines (LNCaP) that do not highly express CD44 (Figure 3A). This important finding motivates CD44 targeting by HA-NPs to induce targeted drug delivery and imaging. Uptake of Cy5.5-labeled HA-NPs by Du-145 and PC3 cells was monitored in vitro (Figure 3B, C). HA-NP uptake saturated within 2 hours of incubation at 50 µg/mL HA-NPs (**Specific Aim 1, Subtask 3**). Analysis is based on in vitro fluorescence microscopy using the protocol in Appendix I.D. However, fluorescence activated cell sorting (FACS) analysis in all cell types, including PrEC cell lines as control, need to be completed for quantitative analysis. DTX was effectively loaded into the core of HA-NPs with about a 18% loading content, but doxorubicin (DOX) had greater loading content and was pursued as a drug model (**Table 1**, Specific Aim 2, Subtask 1-2).

Samples	**Loading content (%)**	**Loading efficiency (%)**	**Mean diameter (nm)**	**Zeta potential (mV)**
HA-NPs	-	-	238.3 ± 2.3	-31.4 ± 0.6
DOX-loaded HA-NPs	21.4 ± 1.6	71.3 ± 5.4	206.4 ± 8.1	-20 ± 2.7

Table 1. Diameter measurements of HA-NPs and DOX-loaded HA-NPs. HA-NP measurements included in reference (Appendix II): Y. Oh,* M. Swierczewska,* et al. Journal of Controlled Release (2015) DOI: 10.1016/j.jconrel.2015.09.014.

DTX-loaded, Cy5.5-labeled HA-NPs were treated to prostate cancer and control cells in cell culture. PC3 and DU145 cell took up HA-NPs within 30 minutes after incubation (Figure 3C). On the other hand, HEK293T cells, which shows low CD44 expression levels, demonstrates limited uptake of drug-loaded HA-NPs based on its preserved viability over drug along (Figure 3C).

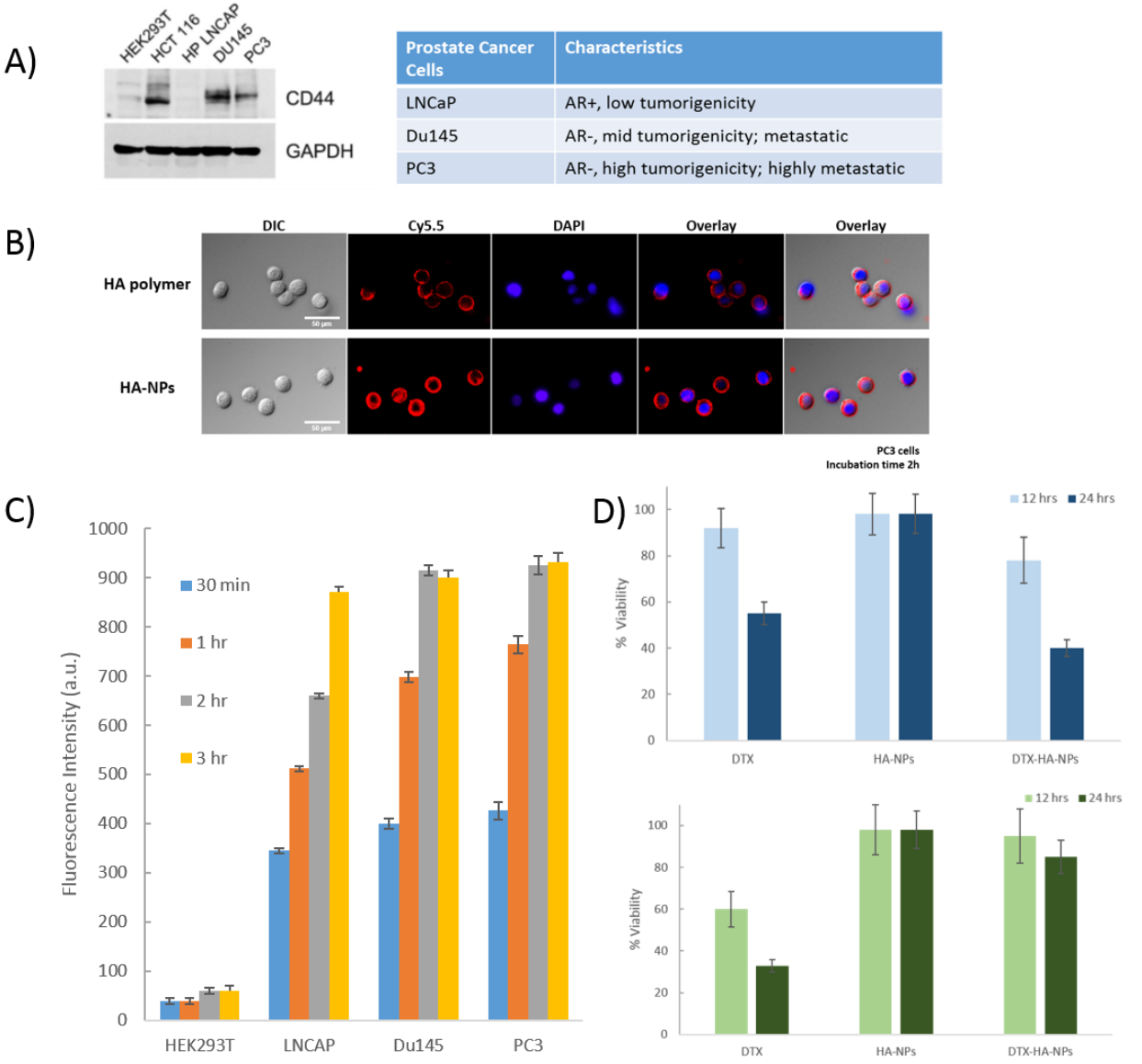

Figure 3. CD44-mediated HA-NP uptake. A) CD44 receptor expression levels measured by western blot (left) in prostate cancer cell lines PC3, DU145, and LNCaP, correlated with their tumorigenic and metastatic properties (right). B) Cy5.5-labeled HA-NPs (50 µg/mL) or HA polymer (234.4 kDa) were incubated for 2 hours with PC3 cells. C) Quantitative image analysis of Cy5.5 signal in HEK293T, LNCAP, PC3 and DU145 cells after incubating Cy5.5-labeled HA-NPs (50 µg/mL) at various incubation times. Fluorescence mean ± S.D., 500 cells. D) Cell viability of PC3 (top, blue) and HEK293T cells (bottom, green) after 12 and 24 hour incubation with DTX-loaded HA-NPs (DTX-HA-NPs), bare Cy5.5-labeled HA-NPs (HA-NPs) and free drug (DTX) measured by MTT assays. DTX concentration was normalized among groups. PC cells: 3 uM DTX, HEK293T cells: DTX 30 nM DTX. Cell viability mean ± S.D., 3 independent experiences performed in triplicate. Percent viability compared to untreated cells.

The major activities completed in Year 1 focused on chemical synthesis, namely Subtasks 1 of Specific Aims 1 and 2 and drug-loaded HA-nanoparticles (HA-NPs) related to Specific Aim 2 Subtasks 1-3.

Year 2:

Year 2 studies focused on the in vivo performance of the nanoparticles developed in Year 1. Near infrared fluorescence (NIRF) in vivo and ex vivo imaging of activatable HA-NPs was applied to demonstrate particle distribution in PC-3 tumor-bearing mice. PC-3 tumor model was prepared by subcutaneously injecting a suspension of 1 x 10^6 PC3 cells in saline in the front flank of athymic nude mice, which were eight weeks old. Nanoparticles were injected intravenously into the mice when the tumor size reached 100 mm^3. In vivo fluorescence intensity was sufficiently detected with an initial dose of 4 mg/kg of HA-NPs, which was based on previous studies of non-activatable particles (Choi, et al. J.Mater.Chem. 2009, 19, 4102–4107). Fluorophore (Cy5.5) labeled HA polymer was synthesized and compared with HA-NPs at the same dose. Fluorescence intensity was monitored starting at 1 hour post-injection (Figure 4). After 24 hours, major organs and tumor were excised from the mice and NIRF imaging was performed to detect fluorescence signals from th particles and HA polymer (Figure 5, left). For ex vivo imaging, NIRF was quantified at a region of interest (ROI). The quantified fluorescent intensities for three animals are expressed as means +/- SD (Figure 5, right).

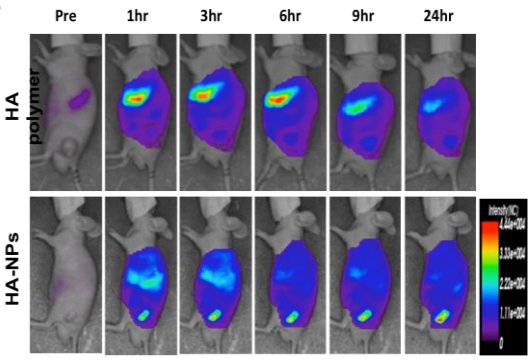

Figure 4: In vivo optical imaging of PC3 tumor-bearing mice treated with Cy5.5 labeled HA (234 kDa; top) or activatable HA-NPs (234 kDa HA, bottom), i.v.

Liver, lung and kidney are the major organs that tend to come in contact with nanopaticles after systemic administration. These tissues along with the tumor were analyzed for CD44 expression by immunohistochemistry (Figure 6). Because HA-NPs target CD44 receptors for cell uptake (Specific Aim 2), it is hypothesized that the particles will be preferentially takem up by the tissue that has the greatest CD44 expression. Immunohistochemistry demonstrates that the tumor tissue had much greater CD44 expression, in lign with the in vivo and ex vivo NIRF imaging.

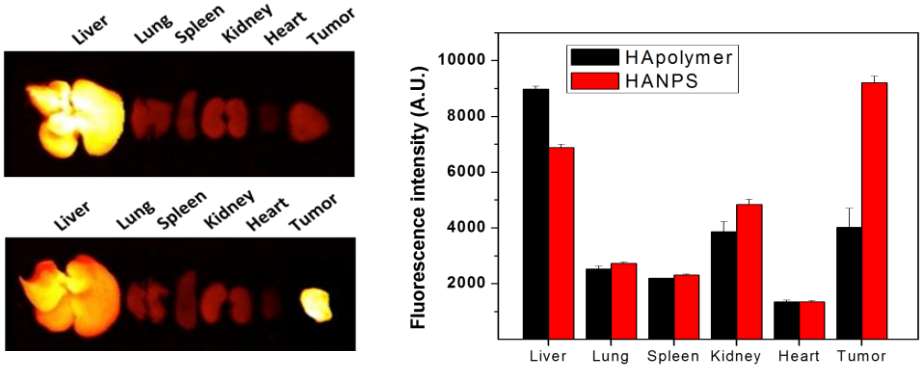

Figure 5: Ex vivo optical imaging (left) and fluorescence quantification (right) of PC3 tumor-bearing mice treated with Cy5.5 labeled HA (234 kDa; top) or activatable HA-NPs (234 kDa HA, bottom), i.v.

The major activities completed in Year 2 focused on the biodistribution of the particles, namely Subtask 3 of Specific Aims 3. These proof-of-concept studies demonstrate that HA-NPs can target PC-3 prostate cancer tumors in mice models and indicate the tumor location by NIRF (an imaging technique translatable to intravital imaging) – a theranostic approach. However, it is important to demonstrate the therapeutic efficacy of the drug delivery, ideally as a survival study.

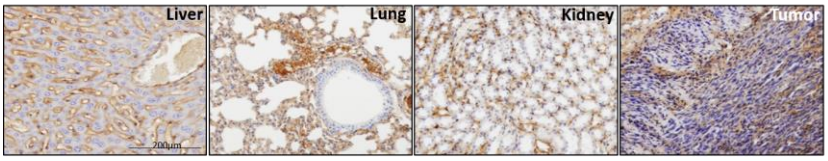

Figure 6: CD44 tissue immunochemistry from PC3 tumor bearing mice treated with HA-NPs, i.v. CD44 = purple

Together Year 1 and 2 studies support the hypothesis that the HA-based nanoformulation can target prostate tumor, and enter prostate cancer cell through HA-CD44 interactions. Once HA-NF is intracellularly delivered, 1) the HA backbone is metabolized by HYAL1 causing the 2) loaded drug in the HA-NF to escape in the intracellular space and causing the 3) dye and quencher pairs to part allowing fluorescence to recover. However, because Year 2 studies were cut short because I took a position at the Nanotehnology Characterization Lab and the planned studies took much longer to accomplish, all the specific aims could not be achieved. Future studies are continued in the lab of Dr. Seulki Lee. Essential studies to be completed include radiolabeling of HA-based nanoformulation to perform PET imaging and determine the injected dose in the tumor. This will provide a measure of how much nanoparticles can enter the tumor in order to estimate how much particle much reach a tumor for effective therapeutic and diagnostic effects. More importantly, an orthotopic metastatic prostate cancer model, unlike xenograft tumor models, provides an accurate picture of the tumor microenvironment. This subcutaneous tumor model is an initial validation system for tumor targeted delivery. Most importantly, a metastatic tumor prostate cancer model needs to be investigated to indicate if the particles can detect and deliver drug to metastatic sites.

c) Training and Professional Development

- I met extensively with my mentors, Dr. Pomper and Dr. Lee, during this year. With their introductions, I met with clinicians with expertise not only in prostate cancer but other disease indications. I was able to participate in an important discussion with biotechnology professionals, manufacturing experts, clinicians and entrepreneurs to discuss clinical translation of a lead biologic drug and the development of clinical trial protocols. I was able to pick up the important aspects of translating a therapeutic and the important decisions that must be made when deciding on clinical endpoints.

- I attended weekly meetings in Dr. Pomper's group. Meetings extensively cover translational science and clinical research.

- Furthermore, I attended biotechnology career development programs through Johns Hopkins' Biomedical Careers Initiative that allowed me to discuss clinical translation with entrepreneurs and professionals in the biotechnology field.

- I was selected as one of the top 50 future biotech leaders in the Mid-Atlantic Region to attend the inaugural 2015 Leaders of Tomorrow Summit during the MD Regional Biotech Forum. This meeting covered key skills that are required to enter the biotechnology field and culminated with a plenary talk by Dr. Pascal Soriot, the CEO of AstraZeneca.

- I discussed my career goals with Dr. Lee and gained extensive knowledge on how to transition my skills to a permanent position. I accepted a Technical Writer position at the Nanotechnology Characterization Lab (NCL) as a Leidos Biomedical Research, Inc. employee.

d) Results Disseminated to Communities of Interest

I presented my research results and research plans to Dr. Pomper's and Dr. Hanes's lab group. Because of the large interdisciplinary group, consisting of clinicians and clinician-scientists, I received advice on my work from numerous lab members.

I presented my work as a poster at the 2015 World Molecular Imaging Congress (WMIC) held on September 2-5, 2015 in Honolulu, Hawaii. During the meeting, I presented my work with other researchers in the imaging field. Discussions also focused on the field of precision medicine overall, which was the theme of WMIC 2015.

e) Plans for Next Reporting Period

Nothing to report.

4. IMPACT

a) Impact on Development of the Principal Disciplines

The results utilize nanotechnology and molecular imaging to develop 1) an activatable probe indicating the HA metabolism of prostate cancer cells and 2) a therapy using targeted HA-based nanoparticles that serve as targeted, drug delivery agents. By developing these molecular-sensitive nanoparticles, additional targeted and sensitive applications of nanomedicine may be envisioned. The goal of the project was to develop a tumor-homing, biomaterial-based diagnostic and drug delivery system that can activate fluorescence and then release an anticancer drug when the prostate cancer environment enters a potential metastatic state. Results indicate that the fluorescence signals can indicate changes in the prostate cancer environment based on hyaluronidase levels, which has not be carefully monitored in previous studies. This technique may allow researchers to study the progression of prostate cancer in animal models, which can greatly advance drug design and development. The drug delivery platform provides the clinical field with a targeted delivery approach of second-line therapies, drastically reducing side effects especially in the elderly. Overall, these results motivate additional studies and ideas of molecularly-responsive nanomedicines for the selective treatment of other disorders.

b) Impact on Other Disciplines

Nothing to Report.

c) Impact on Technology Transfer

If these carbohydrate-based signal-emitting, drug carriers show effective monitoring and treatment of metastatic prostate cancer in vivo, the theranostic application of HA-NPs may be patent-worthy. No intellectual property was filed regarding this specific technology.

d) Impact on Society Beyond Science and Technology

Although significant advancements have been made in the detection and diagnosis of prostate cancer, it remains the second leading cause of cancer death in American men. About 1 man in 6 will be diagnosed with prostate cancer and about 1 of 36 diagnosed will die of prostate cancer. A significant challenge in prostate cancer after relapse to first-line therapy is that metastasis may occur without any prior indicators. This makes prostate cancer progression difficult to predict. It is now accepted that human prostate cancer progression can be predicted by the imbalance between hyaluronan (HA) and the HA-degrading enzyme, hyaluronidase 1

(HYAL1), resulting in high concentrations of each molecule. With the completion of this study, a unique diagnostic and therapeutic nano-platform will be introduced into the research and preclinical field of prostate cancer. With additional studies, the platform can be translated to patients and serve as a dual (a) indicator of prostate cancer metastasis as well as a (b) provider of an immediate therapeutic response to metastasis.

5. CHANGES/PROBLEMS

a) Changes in Approach and Reasons for Change

Nothing to Report.

b) Actual or Anticipated Problems or Delays

Significant delays occurred when optimizing the technology to in vivo studies. Radio labeling proved time-consuming and was not performed during the limited time in Year 2. Long-term survival studies were not started because of limited time. This study was terminated early because the PI moved to a different job.

c) Changes that had a Significant Impact on Expenditures

Nothing to Report.

d) Significant Changes in Use/Care of Vertebrate Animals, Biohazards, and/or Select Agents

Nothing to Report.

6. PRODUCTS

a) Journal Manuscripts Under Review

Nothing to Report.

b) Articles In Press

- Y. Oh,* M. Swierczewska,* et al. Delivery of Tumor-Homing TRAIL Sensitizer with Long-acting TRAIL as a Theraly for TRAIL-resistant Tumors, Journal of Controlled Release (2015) DOI: 10.1016/j.jconrel.2015.09.014 * contributed equally
- M. Swierczewska, H.S. Han, K. Kim, J.H. Park, S. Lee. Polysaccharide-based Nanoparticles for Theranostic Nanomedicine, Advanced Drug Delivery Reviews, 99 (Pt A), 70-84. DOI: 10.1016/j.addr.2015.11.015

Both articles acknowledge the federal support of the DOD PCRP program.

c) Poster Presentation

Abstract Title: Hyaluronic Acid-Based Nanoplatform for Prostate Cancer Therapy
World Molecular Imaging Congress (WMIC) 2015 Meeting, September 2-5, 2014, Honolulu, Hawaii
Session Date/Time: September 5, 2015 from 1:45 PM to 2:45 PM

d) Inventions, Patent Applications, and/or Licenses

Nothing to Report.

7. PARTICIPANTS & OTHER COLLABORATING ORGANIZATIONS

e) Individuals Worked on the Project

No Change from Proposal.

f) Change in Active Other Support of the PD/PI(s) or Senior/Key Personnel

Nothing to Report.

g) Other organizations Involved as Partners

Nothing to Report.

8. SPECIAL REPORTING REQUIREMENTS

Not Applicable.

9. APPENDIX

Appendix I. Optimized Protocols

A. Synthesis of hydrophobically-modified HA

The hydrophobic moiety, 5-beta cholanic acid, is conjugated to the 234 kDa HA backbone via EDC/NHS chemistry, as described in Choi, et al. 2009, *J. Mater. Chem.* 19, 4102-7. 5-beta-cholanic acid is converted to aminoethyl 5beta-cholanoamine (EtCA) by dissolving in methanol, and then mixing with concentrated hydrochloride acid. The solution is stirred under reflex for 6 h at 60°C, after which it is cooled to 0°C and precipitated, filtered, and washed with methanol. The product was dried in a vacuum in room temperature to obtain 5beta-cholanic acid methyl ester. Then it is dissolved in ethylenediamine and refluxed for 6 h at 130°C. The solution was cooled to room temperature until precipitation which are filtered through a membrane filter and washed with water. The EtCA is dried in a vacuum and characterized using ^{1}H NMR. EtCA was then conjugated to the carboxylic acids of HA via EDC and NHS chemistry. EtCA dissolved in DMF is slowly added to a solution of sodium hyaluronate dissolved in formamide containing EDC and NHS and finally mixed for one day. The resulting solution is dialyzed against excess amount of water/methanol for 1 day and distilled water for 2 days. The compound is finally freeze-dried. To characterize the conjugates, the samples are dissolved in D_2O/CD_3OD (1:1, v/v) and analyzed by ^{1}H NMR.

B. Conjugation of Cy.5.5 and BHQ3 to hydrophobically-modified HA

BHQ3 NHS ester and Cy5.5 NHS ester at a 2:1 molar ratio is conjugated via EDC/NHS chemistry. HA-CA is chemically modified with an amine using adipic acid dihydrazide (ADH) in the presence of EDC and 1-hydroxybenzotriazole (HOBt). The HA-amine derivative is then reacted with Cy5.5 NHS ester and BHQ3 NHS ester, as described in Bulputt, P and D. Aeschlimann, *J. Biomed. Mater. Res*. 1999, vol. 47, 152-69 (Figure Appendix I.1). The efficacy of Cy5.5 and BHQ3 conjugation to HA is determined using UV/Vis spectrophotometer at 680 nm and 672 nm absorbance, respectively, using absorbance-concentration curves.

C. DTX loading into HA-Nanoformulation (HA-NF)

To prepare the nanoformulation, the HA-CA conjugates are dissolved in PBS and homogenized in a bench-top high pressure homogenizer (Avestin EmulsiFlex-B15) for at least tem passes. The solution is filtered through a membrane filter with a pore size of 0.45 um. The nanoparticles are characterized using a commercial zeta-sizer.

D. Monitoring cellular uptake of HA-NF

PCa cell lines **(**LNCaP, DU-145, PC-3) and non-cancerous cell lines PrEC. LNCaP is cultured in RPMI media, DU-145 in Eagle's Minimum Essential Medium, and PC3 cells in F-12K Medium. Cell media is supplemented with 10% fetal bovine serum, 10 Units/mL penicillin and 10 ug/mL streptomycin. All cells will be incubated in a 5% CO2 atmosphere and 95% relative humidity at 37°C. Uptake of HA-NFs will be monitored by microscopy. Cells are seeded at a density of 1.0 x 10^5 cells per well of a 4 chamber slide. After 24 h incubation, the cell culture media is removed and replaced with media and 0-100 ug/mL of HA-NF for at least 2 hours. After incubation, all media is removed and cells are washed with PBS at least 3 times. The cells are fixed for 4% formaldehyde solution for 10 mins and dried completely. VETASHIELD mounting medium with DAPI is added to prevent fading and stain the nuclei. The stained cells will be monitored by fluorescence microscopy for DAPI (ex/em: 358 nm/461 nm) and Cy5.5 (ex/em: 675 nm/695 nm) and images analyzed by ImageJ.

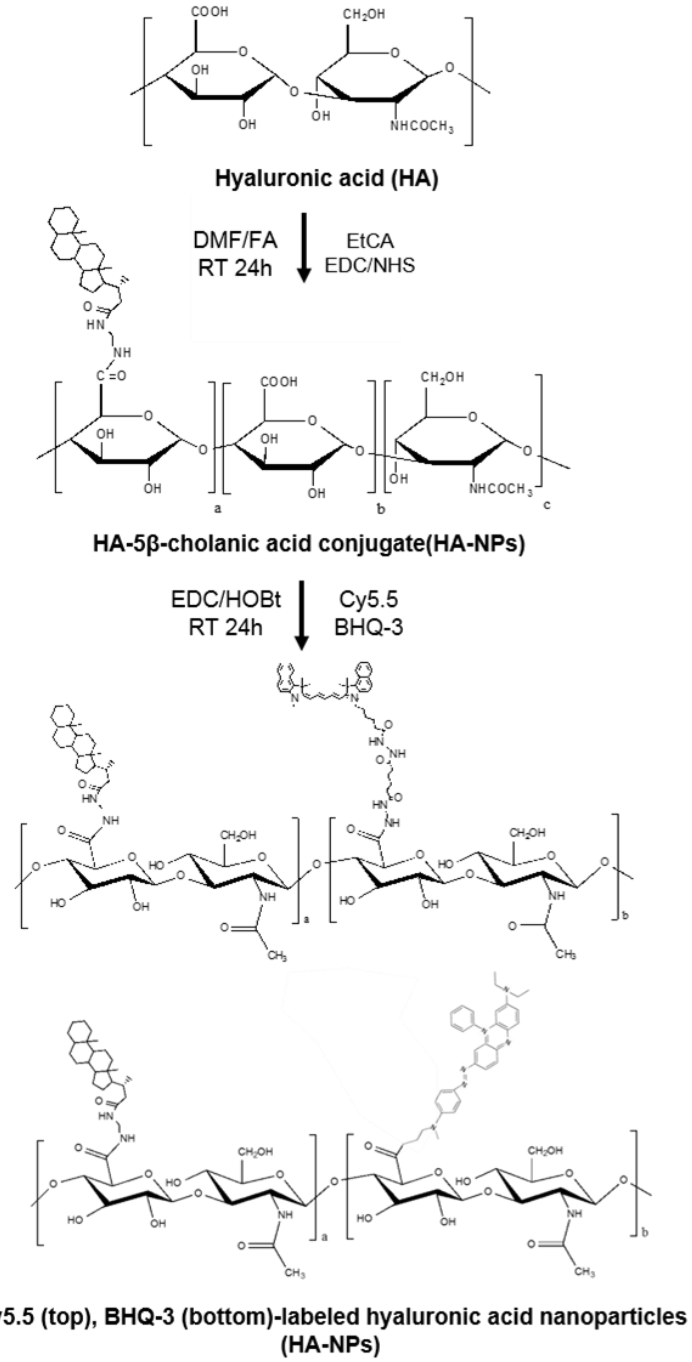

Figure Appendix I.1. Schematic describing conjugation of Cy5.5 and BHQ3 to HACA.

Appendix II. Publication that utilized HA-NPs loaded with doxorubicin for tumor-homing in colon cancer animal model.

Y. Oh,* M. Swierczewska,* et al. Delivery of Tumor-Homing TRAIL Sensitizer with Long-acting TRAIL as a Theraly for TRAIL-resistant Tumors, Journal of Controlled Release (2015) DOI: 10.1016/j.jconrel.2015.09.014.

HHS Public Access

Author manuscript

J Control Release. Author manuscript; available in PMC 2016 December 28.

Published in final edited form as:

J Control Release. 2015 December 28; 220(0 0): 671–681. doi:10.1016/j.jconrel.2015.09.014.

Delivery of tumor-homing TRAIL sensitizer with long-acting TRAIL as a therapy for TRAIL-resistant tumors

Yumin Oh[a,b,1], **Magdalena Swierczewska**[a,b,1], **Tae Hyung Kim**[a,b], **Sung Mook Lim**[c], **Ha Na Eom**[c], **Jae Hyung Park**[d], **Dong Hee Na**[e], **Kwangmeyung Kim**[f], **Kang Choon Lee**[c], **Martin G. Pomper**[a,g], and **Seulki Lee**[a,b,g,*]

[a]Russell H. Morgan Department of Radiology and Radiological Science, Johns Hopkins School of Medicine, Baltimore, Maryland, USA

[b]Center for Nanomedicine at the Wilmer Eye Institute, Johns Hopkins School of Medicine, Baltimore, Maryland, USA

[c]College of Pharmacy, Sungkyunkwan University, Suwon, Korea

[d]Department of Polymer Science and Engineering, Sungkyunkwan University, Suwon, Korea

[e]College of Pharmacy and Research Institute of Pharmaceutical Sciences, Kyungpook National University, Daegu, Korea

[f]Center for Theragnosis, Korea Institute of Science of Technology, Seoul, Korea

[g]Department of Materials Science and Engineering, Johns Hopkins University, Baltimore, Maryland, USA

Abstract

Tumor necrosis factor-related apoptosis inducing ligand (TRAIL) has attracted great interest as a cancer therapy because it selectively induces death receptor (DR)-mediated apoptosis in cancer cells while sparing normal tissue. However, recombinant human TRAIL demonstrates limited therapeutic efficacy in clinical trials, possibly due to TRAIL-resistance of primary cancers and its inherent short half-life. Here we introduce drug delivery approaches to maximize in vivo potency of TRAIL in TRAIL-resistant tumor xenografts by (1) extending the half-life of the ligand with PEGylated TRAIL ($TRAIL_{PEG}$) and (2) concentrating a TRAIL sensitizer, selected from in vitro screening, in tumors via tumor-homing nanoparticles. Antitumor efficacy of $TRAIL_{PEG}$ with tumor-homing sensitizer was evaluated in HCT116 and HT-29 colon xenografts. Western blot, real-time PCR, immunohistochemistry and cell viability assays were employed to investigate mechanisms of action and antitumor efficacy of the combination. We discovered that doxorubicin (DOX) sensitizes TRAIL-resistant HT-29 colon cancer cells to TRAIL by upregulating mRNA expression of DR5 by 60% in vitro. Intravenously administered free DOX does not effectively

*Corresponding author: seulki@jhmi.edu.

[1]These authors contributed equally to this work.

Disclosure of Potential Conflicts of Interest: No potential conflicts of interest were disclosed.

upregulate DR5 in tumor tissues nor demonstrate synergy with $TRAIL_{PEG}$ in HT-29 xenografts, but rather introduces significant systemic toxicity. Alternatively, when DOX was encapsulated in hyaluronic acid-based nanoparticles (HAC/DOX) and intravenously administered with $TRAIL_{PEG}$, DR-mediated apoptosis was potentiated in HT-29 tumors by upregulating DR5 protein expression by 70% and initiating both extrinsic and intrinsic apoptotic pathways with reduced systemic toxicity compared to HAC/DOX or free DOX combined with $TRAIL_{PEG}$ (80% vs. 40% survival rate; 75% vs. 34% tumor growth inhibition). This study demonstrates a unique approach to overcome TRAIL-based therapy drawbacks using sequential administration of a tumor-homing TRAIL sensitizer and long-acting $TRAIL_{PEG}$.

Graphical abstract

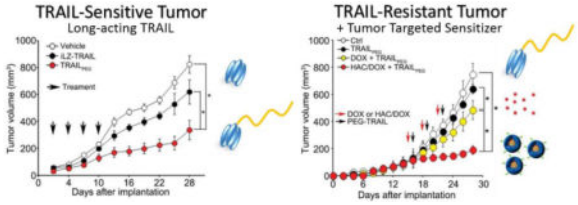

Keywords

apoptosis; death receptors; nanomedicine; TRAIL; TRAIL sensitizers

1. Introduction

Recombinant human tumor necrosis factor (TNF)-related apoptosis inducing ligand (rhTRAIL) and its agonistic antibodies have been under intense focus as crucial, molecularly targeted, antitumor biologics [1, 2]. Unlike conventional anticancer agents and even other TNF family members, rhTRAIL selectively transduces apoptotic signals by binding to death receptors (DRs) that are widely expressed in most cancers, TRAIL-R1/DR4 and TRAIL-R2/DR5, while sparing normal cells [3–5]. This high tumor specificity along with broad applicability across multiple cancer types and proven safety in humans make TRAIL an ideal candidate for cancer therapy [6–8]. However, recent clinical trials of rhTRAIL, e.g. dulanermin, or humanized DR agonistic monoclonal antibodies, tested as either a monotherapy or combined with anticancer agents have failed to demonstrate benefits in cancer patients compared with historical controls [9–12]. The disappointing results raise concerns for the therapeutic implications of rhTRAIL. We identify two challenges that need to be overcome to adapt TRAIL-based agents as therapeutics – natural resistance and poor pharmacokinetics. We address these challenges using a drug delivery strategy with a targeted drug carrier and modified form of TRAIL.

The primary challenge to tackle in TRAIL-based therapy is natural resistance. The majority of primary cancer cells are TRAIL-resistant [11–13]. Mechanisms of TRAIL resistance are distinct among cancer cell types; however, they commonly comprise of: reduced cell surface DR expression, inhibited caspase-8 activation - the initiator caspase, up-regulated anti-apoptotic molecules such as Bcl-2 and the inhibitors of apoptosis (IAP) family proteins, and reduced expression of pro-apoptotic proteins like Bax/Bak [14, 15]. The role of diverse

molecules like anticancer agents and natural compounds in sensitizing TRAIL-resistant cancer cells has been investigated and introduced as an addition to TRAIL monotherapy. TRAIL-based combinations were well validated in vitro and in a few in vivo cancer models; however, they fail to demonstrate a similar synergy in cancer patients. Many reported examples utilize very high doses of chemotherapeutics for TRAIL sensitization that are limited for in vivo application in both dosing frequency and toxicity. This implies a need for alternative approaches to enable rhTRAIL combination therapy in the clinic. In this report, we utilize targeted drug carriers to achieve appropriate TRAIL sensitizer accumulation directly at the site of action.

In addition to TRAIL-resistance, rhTRAIL has an extremely short half-life in physiological conditions, 3–5 min in rodents and less than 30 min in humans [16, 17]. It is widely accepted that wild-type proteins with short half-lives do not exhibit similar biological potency in physiological conditions as those tested in vitro [18]. Use of a more stable form of rhTRAIL with an extended half-life is expected to improve TRAIL action in physiological conditions, particularly for a biologic with an exceptionally short half-life like TRAIL. We firstly developed a series of long-acting PEGylated TRAILs ($TRAIL_{PEG}$) by PEGylating an isoleucine-zipper-fused TRAIL (iLZ-TRAIL), a TRAIL variant that is known to be more potent than rhTRAIL [19]. PEGylation is considered the gold standard for half-life extension and a highly efficient commercial strategy as proven by PEGylated interferons and other FDA-approved biologics [20]. $TRAIL_{PEG}$ has increased stability over rhTRAIL with a significantly longer circulation half-life in rats [21, 22]. As a result, $TRAIL_{PEG}$ demonstrated superior in vivo anticancer potencies in xenografts bearing TRAIL-sensitive HCT116 colon cancer tumors over iLZ-TRAIL. Increasing the circulation time of TRAIL is still not a solution for targeting primary tumors associated with TRAIL resistance at the molecular level.

By integrating recent findings from basic and clinical studies in TRAIL biology and therapy, we hypothesize that TRAIL can have clinical efficacy in cancer by simultaneously addressing two key limitations, TRAIL resistance and its short half-life. First, we selected a TRAIL sensitizer in TRAIL-resistant colon cancer cells through cell-based screening and explored TRAIL and apoptotic signals at the molecular level. Next, the selected TRAIL sensitizer alone or formulated with tumor-homing polymer nanoparticles were systemically administered to xenografts bearing TRAIL-resistant tumors followed by $TRAIL_{PEG}$ administration to investigate a synergistic effect on TRAIL-induced apoptosis in vivo. Lastly, we show the necessary conditions to potentiate anticancer efficacy of TRAIL with a select, tumor-homing TRAIL sensitizer and TRAIL variant in vivo. These studies demonstrate that strategies that address the short half-life of TRAIL alone or TRAIL resistance alone are not effective and hence may explain the disappointing clinical results of TRAIL-based cancer therapies thus far. Rather, a broad approach of addressing the two key TRAIL disadvantages can provide insight towards a viable clinical option for TRAIL-based therapies.

2. Material and Methods

2.1. In Vitro Studies of $TRAIL_{PEG}$ Sensitivity in Human Cancer Cell Lines

2.1.1. Cell Culture—HT-29, SW620, HCT116, and MDA-MB-231 cells were maintained in RPMI 1640 medium (Sigma, St. Louis, MO) supplemented with 10% fetal bovine serum (FBS; Life Technology, Carlsbad, CA), 1% penicillin, and 1% streptomycin (Life Technology). Cells were cultured at 37°C under an atmosphere of 5% CO_2. PC-3 and A549 cells were maintained in F-12K medium (Sigma) supplemented with 10% FBS, 1% penicillin, and 1% streptomycin. HEK293T cells were cultured in Modified Eagles Medium (MEM) (Sigma) supplemented with 10% FBS, 1% penicillin, and 1% streptomycin. These cell lines were purchased from ATCC (Manassas, VA). The cell lines were not authenticated was by the authors. Typically, 2×10^5 cells per well were plated in 6-well plates for treatment of agents.

2.1.2. Cell Viability—A total of 1×10^4 cells were plated in 0.1 mL in 96-well flat bottom plates and incubated for 24h before being exposed to various stimuli. After incubation for the indicated times, 5 μg/mL MTT solution was added to each well and incubated for 1 h. After removal of the medium, 200 μL of DMSO was added to each well to dissolve the formazan crystals. The absorbance at 540 nm was determined using a microplate reader (Bio-Tek Instruments, Inc, Winooski, VT). Triplicate wells were assayed for each condition.

2.2 TRAIL Signaling and Apoptosis Analysis

2.2.1. In Situ DNA Strand Break Labeling (TUNEL assay)—Tumor tissues were recovered from euthanized animals. Sections (5 μm) were cut from 10% neutral buffered, formalin-fixed, paraffin- embedded tissue blocks. Apoptotic cell death in tumor tissues was visualized by performing TdT-mediated dUTP nick end labeling (TUNEL) assays according to the manufacturer instructions (Roche Mannheim, Germany).

2.2.2. Antibodies and Western Blotting—Anti-caspase-8 (Cell Signaling Technology, Danvers, MA, #9746), anti-cleaved PARP-1 (Cell Signaling Technology, #5625), anti-cleaved caspase-3 (Cell Signaling Technology, #9664), anti-cleaved caspase-9 (Cell Signaling Technology, #7237), anti-CD44 (Cell Signaling Technology, #5640), anti-p-JNK (Cell Signaling Technology, #4668), anti-p-p53 (Ser15 Cell Signaling Technology, #9284), anti-BCl-2 (Cell Signaling Technology, #2870), anti-p-BCL-2 (Cell Signaling Technology, #2875), anti-BCL-XL (Cell Signaling Technology, #2764), anti-DR4 (Abcam, Cambridge, MA, #13890), anti-DR5 (Abcam, #47179), anti-c-Jun (Santa Cruz Biotechnology, Santa Cruz, CA, sc-1694), or anti-β-actin (sc-47778) were used in Western blot analysis. In general, cells were lyzed and sonicated briefly in ice-cold PBS buffer (1 mM PMSF, and 1 μg/ml each of aprotinin, leupeptin, and pepstatin A). Cell lysates were clarified by centrifugation, resolved by SDS-PAGE, and proteins on gels were transferred to nitrocellulose (Bio-Rad, Hercules, CA) using a semidry blotter (Bio-Rad). The membrane was blocked with 3% BSA in TBST (10 mM Tris-Cl, pH 8.0, 150 mM NaCl, 0.05% Tween-20) and incubated overnight at 4°C with primary antibodies. Immunoblots were visualized by an enhanced chemiluminescence method and analyzed by Multigauge software (Fujifilm, Tokyo, Japan).

2.2.3. DR5 siRNA Transfection—HT-29 cells were cultured in 6 well plates for 24 h and the cells were transfected with DR5 siRNA (Santa Cruz Biotechnology, Santa Cruz, CA, sc-40237) or control siRNA for 48 h. Transfection was carried out using Lipofectamine 2000 reagent (Invitrogen) following the manufacturer's instructions.

2.2.4. Quantitative RT (reverse transcription)-PCR—Total cellular RNA was purified from HT-29 cells using Trizol reagent (Life Technology) and subjected to amplification with SuperScript One-Step RT–PCR system (Life Technology). Real-time PCR was carried out using a StepOne™ Real-Time PCR System according to the manufacturer instructions (Life Technology). The mean cycle threshold value (Ct) from triplicate samples was used to calculate the gene expression. β-actin was used as an internal control to normalize the variability in expression. Experiment was repeated three times with identical results. The following specific primers sets that are consensus region among isoforms were used for PCR; *DR4*, forward 5′-TGT GAC TTT GGT TGT TCC GTT GC-3′ and reverse 5′-ACC TGA GCC GAT GCA ACA ACA G-3′; *DR5*, forward 5′- AAG ACC CTT GTG CTC GTT GT-3′ and reverse 5′-AGG TGG ACA CAA TCC CTC TG-3′; *actin*, forward 5′- TCC CTG GAG AAG AGC TAC GA-3′ and reverse 5′-AGC ACT GTG TTG GCG TAC AG-3′.

2.2.5. Death-Inducing Signaling Complex Immunoprecipitation—After HT-29 cells achieved 80% confluence, the cells were pretreated with doxorubicin for 24 h and then incubated with 500 ng/mL Flag-TRAIL (Enzo Life Sciences, Farmington, NY) for 30 min at 37°C. The cells were lysed with DISC IP lysis buffer (30 mM Tris, pH 7.4, 150 mM NaCl, 10% glycerol, 1% Triton X-100 with 1 mM PMSF, and 1 μg/mL each of aprotinin, leupeptin, and pepstatin A). Cell lysates were incubated with Flag (M2) beads (Sigma) overnight. The beads were subsequently washed three times with cold PBS, resolved onto SDS-PAGE gels and subjected to Western blot analysis.

2.3 Analysis of TRAIL Sensitizer Cellular Uptake and Tumor Accumulation

2.3.1. Confocal Analysis—HT-29 cells grown on coverslips in 12-well plates were treated with indicated agents. The cells were fixed in 4% paraformaldehyde for 5 min and then washed with ice-cold PBS (pH 8.0) three times. Finally, the cells were mounted on slides for visualization under a Fluoview FV10i-DOC confocal microscope (Olympus Optical, Tokyo, Japan).

2.3.2. Flow Cytometry—Cells were harvested, washed with PBS, re-suspended in 75% ethanol in PBS, and kept at 4°C for 30 min. Cells were re-suspended with 1 mM EDTA, 0.1% Triton-X-100 and 1 mg/ml RNAse A in PBS. The suspension was then analyzed on a FACSCaliber. The histogram in Fig. S4 was generated using the MultiCycle software (Phoenix Flow Systems, San Diego, CA, USA).

2.3.3. DOX Distribution in HT-29 Xenograft Tumors—Mice bearing HT-29 xenograft tumors were intravenously administered with DOX (7 mg/kg) and HAC/DOX (containing 7 mg/kg equivalent doxorubicin) when tumors reached 300 mm^3. At each selected time point, 3 mice in one group were euthanized by cervical dislocation. Whole

blood was collected via cardiac puncture with a heparinized syringe. Tumors were dissected out and frozen at −70°C immediately. Plasma samples were isolated from whole blood by centrifugation at 3000 g for 5 min. Tissues homogenates were prepared in 800 μL water using a Polytron homogenizer (Brinkman Instruments, Mississauga, Ontario, Canada), and then 200 μL of H_2SO_4 was added to the tissue homogenates. The solutions were then digested for 2 h at 60°C. After the vials cooled to room temperature, 100 μL of $AgNO_3$ was added. Then the samples were centrifuged at 12,000g for 10 min, and the supernatant was counted in a fluorospectrometer (RF-5301, Shimadzu) at an excitation wavelength of 500 nm and emission wavelength of 558 nm. The concentration of doxorubicin in each tissue was calculated based on a calibration curve. The calibration curve was linear over the 0.02 and 2.00 μg/mL range with a correlation coefficient of $R^2 = 0.9993$.

2.4. In Vivo Efficacy Studies of $TRAIL_{PEG}$ in Xenograft Mice Models

2.4.1. HCT116 Xenograft Model—All experiments involving tumor xenografts were performed according to protocols approved by the Johns Hopkins Animal Care and Use Committee and animal studies were undertaken in accordance with the rules and regulations. Freshly harvested HCT116 cells (3×10^6 cells/mouse) were inoculated s.c. into BALB/c athymic mice (n=5). When tumor volume reached ~50 mm^3, mice were treated with TRAIL (8 mg/kg, i.v.) or $TRAIL_{PEG}$ (8 mg/kg, i.v.) every 3 days for 2 weeks (total 4 times). Tumor volumes were monitored for 30 days after tumor cell administration. Tumor volumes were calculated using longitudinal (L) and transverse (W) diameters using $V = (L*W^2)/2$, and tumor growth inhibition (TGI) percent values were calculated using the formula $TGI\ \% = (1-TV_{sample}/TV_{control}) \times 100$, where TV is tumor volume.

2.4.2. HT-29 Xenograft Model—The antitumor effects of $TRAIL_{PEG}$ after HAC/DOX sensitizing were investigated in HT-29 tumor bearing mice (n=5). Briefly, freshly harvested HT-29 cells (5×10^6 cells/mouse) were inoculated s.c. into BALB/c athymic mice. Treatment was initiated when the tumors reached a mean volume of 150 mm^3. Mice were treated with three rounds of DOX or HAC/DOX (7 mg/kg, i.v.) combined with $TRAIL_{PEG}$ (8 mg/kg, i.v.) for 10 days. The tumors were analyzed and calculated as described above (n=5).

2.5. Statistical Analysis

All data were analyzed by GraphPad Prism 6 (GraphPad Software, La Jolla, CA). Differences between two means were assessed by a paired or unpaired t-test. Differences among multiple means were assessed, as indicated, by one-way ANOVA, followed by Turkey's post-hoc test or by the Student's *t*-test as appropriate. Error bars represent S.D or S.E.M as indicated. *P*-values <0.05 were considered to be significant.

3. Results

3.1. $TRAIL_{PEG}$ improves pharmacokinetics and reduces tumor growth in TRAIL-sensitive tumor xenografts but does not influence apoptosis in TRAIL-resistant tumors

$TRAIL_{PEG}$ engineered with a 20 kDa PEG molecule was synthesized as previously reported and used throughout the study. Earlier PK studies in rodents demonstrate 20kDa $TRAIL_{PEG}$ has a half-life ($t_{1/2}$) of 12.3 ± 2.2 h in mice (intraperitoneal injection), which is over 11-fold

greater than free iLZ-TRAIL [22]. $TRAIL_{PEG}$ also showed a 21-fold increase in area under the curve (AUC) over TRAIL [22]. To compare pharmacodynamics (PD) between iLZ-TRAIL and TRAILPEG, TRAIL variants were intravenously administered every 3 days for a total of 4 times in HCT116 xenografts when the tumor was palpable (50 mm^3) (Fig. 1A). HCT116 is a human colon cancer cell line that is relatively sensitive to TRAIL-induced apoptosis. Compared to iLZ-TRAIL, $TRAIL_{PEG}$ (200 μg, protein-based) showed increased tumor growth inhibition (TGI) values (at day 28 for iLZ-TRAIL and $TRAIL_{PEG}$; 27% and 58%, respectively). At the end of the study, tumor tissues were harvested and apoptotic cells in tumor sections were visualized by TdT-mediated dUTP nick and labeling (TUNEL) assay (Fig. 1B). $TRAIL_{PEG}$ clearly showed tumor cell apoptosis in vivo compared to marginal signs in the iLZ-TRAIL-treated group. Next, we examined if the improved TRAIL stability of $TRAIL_{PEG}$ contributes to apoptosis in TRAIL-resistant tumors. A panel of known TRAIL-resistant human tumor cell lines including colon (HT-29, SW620), prostate (PC3), breast (MDA-MB-231R, MCF7) and lung (A549) as well as TRAIL-sensitive HCT116 and normal human kidney HEK293T cells were incubated with 1 μg/mL of iLZ-TRAIL or $TRAIL_{PEG}$ for 3 h and 24 h in respective media. TRAIL sensitivities were expressed as induced cell death (%), calculated as the percentage relative to the untreated cells, and measured by MTT assays (Fig. S1A and Fig. 1C). $TRAIL_{PEG}$ provoked strong apoptosis only in TRAIL-sensitive HCT116 cells, like iLZ-TRAIL, as evidenced by cleavage of poly(ADP-ribose) polymerase 1 (PARP-1), a substrate of caspase-3 (Fig. S1B). This study validates that improved stability of $TRAIL_{PEG}$ does not alter the DR-mediated apoptosis signaling in TRAIL-resistant tumors; thus, an additional strategy to extend the $t_{1/2}$ of TRAIL is needed to target both TRAIL-sensitive and -resistant tumors in vivo.

3.2. DOX/$TRAIL_{PEG}$ potentiates DR-mediated apoptosis in TRAIL-resistant tumor cells

Accumulating reports suggest that various FDA-approved chemotherapies sensitize cancer cells to TRAIL-induced apoptosis. To identify synergism with $TRAIL_{PEG}$, common DNA damaging agents approved for colon cancer treatment, including doxorubicin (DOX), 5-fluorouracil (5-Fu), cisplatin (CIS), and irinotecan (IRINO), were incubated in TRAIL-resistant HT-29 cells with or without $TRAIL_{PEG}$ and screened for apoptosis. Lower doses of agents (0.5 μg/mL of DOX, CIS; 1 μg/mL of 5-Fu and 0.6 μg/mL of IRINO) were pretreated in HT-29 cells for 24 h followed by an additional 24 h incubation with either drug alone or in combination with $TRAIL_{PEG}$ (1 μg/mL). The low dose of drugs did not induce apoptosis based on the percentage of relative cell death (Fig. S1C). At high toxic doses (> 10 μg/mL), most of the drug-treated cells were dead in 24 h (data not shown). When HT-29 cells were exposed to sublethal doses of DOX (2 μg/mL), 5-FU (10 μg/mL), CIS (2 μg/mL), or IRINO (3 μg/mL) combined with $TRAIL_{PEG}$, enhanced TRAIL-induced apoptosis was observed compared to drug alone (Fig. 2A). Among tested agents, DOX/$TRAIL_{PEG}$ combination clearly enhanced apoptosis through the proteolytic activation of caspase-8 (Casp-8) and caspase-9 (Casp-9) and consequently cleaved PARP-1 in HT-29 cells (Fig. 2B). Treatment of DOX also led to the phosphorylation of p53 and the activation of c-jun, a downstream substrate of c-Jun N-terminal kinase (JNK). Next, DOX/$TRAIL_{PEG}$ combination treatment was examined for enhanced apoptosis in different TRAIL-resistant cells. Individually, $TRAIL_{PEG}$ or DOX failed to induce PARP-1 cleavage in TRAIL-resistant human tumor cell lines, including HT-29, MDA-MB-231R, A549, and PC3. When combined, PARP-1

activation was significant in all TRAIL-resistant and TRAIL-sensitive cell lines examined, (Fig. 2C) and such synergism was exemplified cell death assays (Fig. S1D). To investigate if enhanced apoptosis by DOX/TRAIL$_{PEG}$ is DR-mediated through death-inducing signaling complex (DISC) formation, TRAIL DISC immunoprecipitation (IP) was assessed in HT-29 cells after treatment of DOX, TRAIL$_{PEG}$ or DOX/TRAIL$_{PEG}$ followed by DR4 and DR5 Western blotting (Fig. 2D). Interestingly, TRAIL-induced DISC demonstrated the recruitment of DR5, but not DR4, on the cellular membrane after DOX/TRAIL treatment. To further validate the DR5 specific regulation, we used siRNA to determine DOX–mediated DR5 up-regulation. DR5 was highly induced by DOX treatment in HT-29 cells but did not upregulate with DR5 siRNA transfection followed by DOX treatment (Fig. 2E). As examined by quantitative real-time PCR (qPCR), DOX increased DR5 mRNA by 60% in HT-29 cells compared to untreated cells, whereas DR4 mRNA levels did not change (Fig. 2F).

3.3. DOX/TRAIL$_{PEG}$ accelerates proteolytic activation of caspases through DR5 upregulation in HT-29 cells

It has been reported that HT-29 cells are TRAIL-resistant because of low DR5 expression on the cellular membrane [23, 24]. In other reports, DOX has been demonstrated to sensitize TRAIL-induced apoptosis by affecting the cell surface localization of DR5 in colon cancer cells [25]. To explore how DOX and DOX/TRAIL$_{PEG}$ enhance apoptosis, HT-29 cells were treated with DOX or DOX/TRAIL$_{PEG}$ at different time points. When HT-29 cells were pre-sensitized with DOX (2 μg/mL) and then treated with TRAIL$_{PEG}$ for 24 h, Casp-8 and Casp-3 activated (Fig. 3A and 3B). Regardless of TRAIL$_{PEG}$, DOX upregulated DR5 expression (3 to 4-fold), but not DR4, at the protein level. TRAIL intrinsically binds to both DR4 and DR5, but we have shown that only altered protein expression of DR5 in HT-29 cells plays a critical role in TRAIL-induced apoptosis while DR4 levels remain unchanged. To assess if the enhanced DOX/TRAIL$_{PEG}$-induced apoptosis is due to altered DR5 expression, we synthesized a peptide-based dimeric DR5 antagonist (DR5-A) based on a reported sequence of YCKVILTHRCY [26] (Fig. S2 and Fig. S3A). The neutralizing efficacy of DR5-A was confirmed by treating HCT116 cells with DR5–A (5, 10 μg/mL) and TRAIL$_{PEG}$ or DR5 agonistic antibody (Fig. S3B and Fig S3C). Upon incubation, the DR5-A effectively blocked TRAIL$_{PEG}$-induced apoptosis by neutralizing DR5 as evidenced by the reduced cleavage of Casp-3 and PARP-1. With this antagonistic peptide, we investigated the extent of DR5 expression induced by DOX treatment and its effect on DOX/TRAIL$_{PEG}$-induced apoptosis in HT-29 cells. When TRAIL$_{PEG}$ was co-treated with both DOX and DR5-A to HT-29 cells, cell death evoked by the DOX/TRAIL$_{PEG}$ treatment was significantly inhibited by 70% compared to that of cells without DR5–A treatment (Fig. 3C). Blocking DR5 substantially decreased the proteolytic activation of Casp-8, Capse-9 and PARP-1 cleavage in cells treated with DOX/TRAIL$_{PEG}$ while showing no effect on BCL2/BCL-XL expression that was mainly reduced by DOX (Fig. 3E). It has been reported that JNK mediates DOX- or TRAIL-induced apoptosis in cancer cells [27]. In addition, activation of the JNK pathway leads to DR upregulation in multiple tumor cells including colon cancer [28, 29]. To study this, HT-29 cells were treated with DOX and TRAIL$_{PEG}$ alone or in combination with SP600125 (20 μM), a JNK inhibitor [30]. Consequently, inhibition of JNK phosphorylation reduced DOX and TRAIL$_{PEG}$-induced cell death by 35%

(Fig. 3D) and suppressed proteolytic activation of Casp-8, Casp-9 and PARP-1 cleavages (Fig. 3F). However, SP600125 had no effect on regulating DR5, indicating DOX-induced DR5 upregulation is not stimulated by the JNK pathway. This suggests that JNK partially mediates DOX/$TRAIL_{PEG}$-induced apoptosis but is not involved in DR5 upregulation in HT-29 cells.

3.4. Tumor-homing HAC/DOX but not free DOX accumulates DOX concentration in tumor tissues in vivo

In many cases, select anticancer agents acting as TRAIL sensitizers in vitro were not fully validated in animal models and when in vivo efficacy was demonstrated, relatively high doses of drugs were needed to effectively sensitize TRAIL-resistant tumors in vivo. However, such exceedingly high doses of chemotherapeutic agents as TRAIL sensitizers are not clinically practical. One effective way to utilize such toxic agents as a sensitizer while minimizing systemic toxicity in vivo is using a tumor-homing drug delivery system. We previously optimized a hyaluronic acid-based conjugate (HAC), a tumor-homing nanocarrier system comprised of biocompatible hyaluronic acid, that can deliver small molecules to the intracellular space of cancer cells via CD44 receptors with reduced systemic toxicity [31, 32]. Importantly, this targeted, intracellular delivery was observed and verified in different in vivo cancer models, ranging from colon and melanoma to head and neck [32–37]. In aqueous solutions, the HAC structure can self-assemble into a nanocarrier sequestering the hydrophobic/amphiphilic molecules to the center of the particle. Because of HAC's abundant functional groups, the surface of HAC can be modified with fluorophores or other detectable moieties for tracking and imaging in cells and in vivo [35]. The schematic diagram and chemical structure of HAC is shown in Fig. 4A. CD44 expression and therefore HAC drug delivery is dependent on cell types. Among the tested cells, HT-29, HCT116, MDA-MB-213R and A549 tumor cells express CD44 whereas SW620 and HEK293T cells do not express high levels of CD44 (Fig. 4B). DOX is well-encapsulated within HAC (HAC/DOX) with a high loading content (21%, wt) and loading efficiency (71%) having a mean diameter of 206 nm in PBS (10 mM, pH 7.4) (Table S1 and Fig. S4A). When DOX was incorporated in HAC labeled with fluorescein molecules and treated to HT-29 cells, HAC/DOX showed rapid cellular uptake after 10 min of incubation and saturated at 1 h (Fig. 4C and Fig. S4B). Importantly, HAC/DOX promptly burst releases the incorporated DOX inside the cell, which is supported by the restored quenched fluorescence of DOX based on microscopy images (Fig. S4C). HAC was shown to be non-toxic in our previous studies [32, 36]. The tumor-homing delivery of DOX by HAC was studied in tumor xenograft models. DOX concentration in plasma and tumor tissues was quantified by fluorescence absorbance followed by an extraction process [38]. When HAC/DOX and the same dose of DOX dissolved in saline was intravenously injected in HT-29 xenografts bearing approximately 300 mm^3 tumors, HAC/DOX delivered more DOX in the harvested tumor tissues than free DOX. The concentration of free DOX in the tumor region gradually decreased with time at 6 h post drug administration (Fig. 4D). In contrast, HAC/DOX markedly increased DOX accumulation in the tumor region from 6 h to 24 h and maintained accumulation 48 h post-injection. HAC/DOX demonstrated 12-fold and 55-fold increased accumulation of DOX in isolated tumors at 24 h and 48 h, respectively, compared to that of DOX alone. To confirm DOX distribution in tumors, harvested tumor sections isolated at 48

h were stained with DAPI and visualized by confocal microscopy (Fig. 4E and Fig. S5A). As expected, HAC/DOX treated tissues showed greater DOX accumulation compared to control.

3.5. A tumor-homing HAC/DOX combined with long-acting $TRAIL_{PEG}$ potentiates apoptosis in TRAIL-resistant tumor xenografts with reduced systemic toxicity

After confirming that HAC/DOX predominantly accumulates in tumors in vivo, the next study examined if HAC/DOX and $TRAIL_{PEG}$ combination effectively upregulates DR5 and initiates apoptosis in vivo as demonstrated in vitro. When tumor volumes reached 200 mm^3, HT-29 xenografts were intravenously treated with $TRAIL_{PEG}$, HAC/DOX and HAC/DOX/$TRAIL_{PEG}$ (n=3). Because a caspase cascade was potentiated in HT-29 cells only when DOX was pretreated in the $TRAIL_{PEG}$ treatment (Fig. 2B and 2C), mice were treated with HAC/DOX (7 mg/kg, DOX-based) 24 h before $TRAIL_{PEG}$ treatment. After 24 h of $TRAIL_{PEG}$ treatment, the expression of DR5 and DR4 as well as Casp-8 and Casp-3 were analyzed in harvested tumor tissues. In accordance with cellular studies, HAC/DOX treatment increased the protein expression of DR5 in tumors by 70% in vivo while DR4 levels remained unchanged (Fig. 5A and 5B). In particular, neither HAC/DOX nor $TRAIL_{PEG}$ alone failed to initiate a caspase cascade. Casp-8 and Casp-3 were strongly activated only when the HAC/DOX and $TRAIL_{PEG}$ were co-treated (Fig. 5C). To find a dose range in mice models, two $TRAIL_{PEG}$ formulations with different DOX concentrations, low (2 mg/kg, DOX-based, Dox_{low}) and high (7 mg/kg, close to maximum tolerated dose, Dox_{high}), were injected in HT-29 xenografts when tumor volumes reached 200 mm^3 followed by $TRAIL_{PEG}$ treatment. Each tumor was harvested and analyzed by immunoblotting after 24 h of $TRAIL_{PEG}$ treatment (Fig. S5B). After a single treatment, DOX at the low dose marginally increased the cleaved Casp-9 and Casp-8 but showed some enhanced activation at the high DOX dose. Interestingly, neither low nor high DOX doses alone altered cleaved Casp-3 levels, an indicator of apoptosis. In contrast, HAC/DOX combined with $TRAIL_{PEG}$ clearly initiated the caspase cascade by regulating cleaved Casp-9 and Casp-8 at both low and high DOX doses. HAC/DOX with low and high DOX concentrations significantly enhanced Casp-3 activation compared to DOX alone (for DOX_{low}, DOX_{high}, HAC/DOX_{low}, HAC/DOX_{high} vs. control, 2, 2, 13, and 24-fold) (Fig. S5C). In contrast to in vitro results, free DOX at the high dose was shown to marginally alter cleavage of initiator caspases, Casp-8 and Casp-9, and not executional caspase, Casp-3, when combined with $TRAIL_{PEG}$ in vivo.

After confirming the necessary condition to generate TRAIL-induced apoptosis in $TRAIL_{PEG}$-resistant tumors in vivo, the drug efficacy and safety of the HAC/DOX and $TRAIL_{PEG}$ combination in HT-29 xenografts was examined. rhTRAIL was excluded from the study, because rhTRAIL is less potent then $TRAIL_{PEG}$. DOX and HAC/DOX alone were also ruled out for the in vivo studies, because they do not efficiently induce apoptosis in HT-29 tumor models as presented earlier (Fig. 5). When tumor volumes reached 150 mm^3, mice were intravenously treated with $TRAIL_{PEG}$ alone or with DOX and HAC/DOX at a 7 mg/kg DOX dose every 3 days for a total of 3 times as indicated in Fig. 6A. $TRAIL_{PEG}$ alone marginally altered tumor growth just as was demonstrated by in vitro studies. In contrast, the two $TRAIL_{PEG}$ combinations suppressed tumor growth. TGI values were

significantly decreased by the HAC/DOX and $TRAIL_{PEG}$ combination throughout the study period (at day 28, for $TRAIL_{PEG}$, DOX and $TRAIL_{PEG}$, HAC/DOX and $TRAIL_{PEG}$; 14, 34, and 75% respectively). It should be noted that 60% of mice treated with a high dose of free DOX died during the treatment cycle due to the toxicity of the agent (Fig. 6B). Although carrying the same amount of high dose, HAC/DOX demonstrated a significantly improved tolerability in terms of survival rate, allowing the use of a necessary high dose of TRAIL sensitizer in vivo.

4. Discussion

TRAIL has unique features as a nontoxic anticancer therapy because it selectively induces apoptosis in a wide range of cancers while leaving normal cells unharmed. However, TRAIL-based therapies tested in cancer patients, even when co-treated with anticancer agents, show marginal responses, suggesting a gap in the therapeutic approach between preclinical models and humans [9, 12]. To date, the critical reasons for such disappointing results are not clearly explained in the literature; and, more importantly, there are no clear alternatives to restore such TRAIL-based therapies in the clinic. Based on our studies, we conclude that an effective TRAIL therapy requires: 1) identification of the tumor's TRAIL sensitivity, 2) physiologically stable and active TRAIL-based compound, and 3) tumor-homing drug delivery techniques for TRAIL sensitizers.

One important property usually neglected in the TRAIL research field is its inherent instability in physiological conditions. During the last few years, we put emphasis on the inherent short half-life of rhTRAIL and developed $TRAIL_{PEG}$ analogs with an extended half-life. A stable isoleucine zipper (iLZ)-TRAIL is known to be more potent in vitro and in vivo compared to that of rhTRAIL because of the improved trimeric protein stability induced by the iLZ motif [39]. Additionally, $TRAIL_{PEG}$ offers improved stability and solubility over rhTRAIL and iLZ fusion TRAIL as well as reduced aggregation at high concentrations, which enables easy handling of the protein in solution [21]. Trimeric $TRAIL_{PEG}$ also has advantages over TRAIL agonistic antibodies in terms of safety and activity induced by clustering of DRs to induce DISC formation efficiently. Because $TRAIL_{PEG}$ contains the native-type protein structure and PEGylation reduces immunogenicity of the compound, it is expected to be less immunogenic compared to humanized antibodies. TRAIL signaling is a complicated process associated with binding to multiple receptors, inciting reports of TRAIL's therapeutic potential in disorders other than cancer particularly in inflammatory diseases. Such roles could not be fully realized by utilizing DR antibodies that affect only a few receptors at most. From this point of view, $TRAIL_{PEG}$ could retain the full biological function of an endogenous TRAIL molecule in vivo with a longer half-life. As a result, the full therapeutic potential of TRAIL can be investigated. Therefore, $TRAIL_{PEG}$ shows greater in vivo anticancer activity than iLZ-TRAIL (Fig. 1A, B), despite having a lower potency in vitro (Fig. 1C). Nonetheless, $TRAIL_{PEG}$ showed marginal efficacy, similar to rhTRAIL, in TRAIL-resistant tumors examined in this study; thus, the results indicate a need for an additional strategy to address TRAIL-resistance in vivo.

Diverse anticancer agents have been utilized as TRAIL sensitizers. In addition to their sensitizing roles in TRAIL-resistant tumors, a combinatory TRAIL and anticancer agent would be an ideal regimen for cancer therapy. TRAIL predominantly mediates an extrinsic pathway for apoptosis via the activation of caspase-8 at the DISC. To a lesser degree, TRAIL also mediates the intrinsic pathway of apoptosis that results in the activation of caspase-9 through the release of cytochrome c from the mitochondria and the activation of other pro-apoptotic factors. Because most conventional anticancer drugs induce apoptosis through the intrinsic pathway, the interplay between the extrinsic and intrinsic apoptotic pathways would be an effective rationale for cancer therapy. In reality, however, dulanermin combined with anticancer drugs did not elicit synergistic effects in cancer patients [12]. We hypothesize that the accumulation of the anticancer drug in the tumor was too low to efficiently sensitize TRAIL-resistant tumors in patients. In many cases, high doses of TRAIL sensitizers were used in animal models of TRAIL-resistant tumors to induce a similar effect demonstrated in vitro. Such high dosing profiles are not applicable in the clinic, because they induce serious systemic toxicity. To overcome the limitation, we firstly screened the $TRAIL_{PEG}$ sensitizing efficacy of four widely used anticancer drugs at sublethal doses in TRAIL-resistant HT-29 colon cancer cells (Fig. 2). Based on the relative cell death and levels of cleaved PARP-1, a hallmark of apoptosis, the combination of DOX and $TRAIL_{PEG}$ was selected for further studies. We validated that DOX enhances TRAIL sensitivity in HT-29 cells by upregulating DR5 specifically on the cellular membrane and, when combined with $TRAIL_{PEG,}$ increases Casp-3 cleavage (Fig. 3). Drug delivery by nanoparticles can reduce high dose DOX-induced systemic toxicity over free DOX by preferentially delivering its cargo to tumor tissues. Therefore, we utilized HAC/DOX as a tumor-homing TRAIL sensitizer to deliver DOX to tumor tissues and in turn sensitize tumor cells to TRAIL in vivo (Fig. 4A). HAC is a model platform for delivering cytotoxic agents, because HAC selectively targets tumors through two distinct mechanisms: passively accumulating in tumors through the enhanced permeability and retention (EPR) effect [40] followed by active targeting of CD44, a natural ligand of hyaluronic acid and an antigen overexpressed on various tumors [41]. In vivo, HAC/DOX prolonged DOX activity in the blood and accumulated DOX at higher concentrations in HT-29 tumor tissues after intravenous injection compared to DOX alone (Fig. 4B–E). Tumor-bearing mice were sacrificed after 24 h of drug treatment, and tumor tissues were analyzed for TRAIL sensitization and apoptosis at the molecular level (Fig. 5). Importantly, intravenously administered free DOX at the high dose did not increase Casp-3 activity when combined with $TRAIL_{PEG}$, whereas HAC/DOX clearly initiated the caspase cascade and potentiated TRAIL-induced apoptosis. In particular, both cleaved Casp-8 and Casp-3 were apparent in tumor tissues only when xenografts were simultaneously treated with HAC/DOX and $TRAIL_{PEG}$. Free DOX combined with $TRAIL_{PEG}$ did not efficiently inhibit tumor growth but rather induced significant systemic toxicity (Fig. 6B). In accordance with in vitro and ex vivo study results, HAC/DOX combined with $TRAIL_{PEG}$ clearly inhibited tumor growth in vivo with improved drug tolerability (Fig. 6).

TRAIL's proven safety and inherent cancer-selectivity warrants its potential as an ideal anticancer therapy, especially with reduced adverse effects compared to conventional first-line chemotherapy. The present study introduces one strategy to restore rhTRAIL-based

therapy in the clinic by addressing at least two key limitations from a drug delivery approach; (1) utilizing rhTRAIL with an extended half-life and (2) effectively sensitizing TRAIL-resistant tumors through tumor-homing TRAIL sensitizers. The strategy can be tailored to include diverse TRAIL sensitizers, reported or novel, formulated with other types of tumor-homing nanoparticles, including nanoparticles in the clinical pipeline [42, 43]. It remains to be investigated if the proposed strategy improves therapeutic efficacy in xenografts bearing different TRAIL-resistant tumor cells and metastatic tumors as well as in patient-derived xenograft models. Based on the high unmet clinical need for effective, less toxic anticancer therapies combined with the unique features of TRAIL in safety and applicability towards many cancer types, we anticipate that new TRAIL-based therapies could benefit cancer patients in the clinic. In our studies, we address two key limitations to first-generation TRAIL-based therapies in order to pave a path towards more promising clinical trials.

5. Conclusion

TRAIL's proven safety and inherent cancer-selectivity retains its potential as an ideal anticancer therapy, despite sobering clinical trials of recombinant TRAIL and more recent TRAIL receptor agonists. By integrating recent findings from clinical and basic science studies, this paper introduces a unique approach to initiate DR-mediated apoptosis in TRAIL-resistant tumors by simultaneously utilizing (1) a long-acting PEGylated iLZ-TRAIL to overcome the short half-life of TRAIL and (2) tumor-homing nanoparticles carrying chemotherapeutic agents as a TRAIL sensitizer to enable efficient TRAIL sensitization of tumors with low systemic toxicity. Our drug delivery strategy may warrant the resurgence of TRAIL-based therapies for clinical translation.

Supplementary Material

Refer to Web version on PubMed Central for supplementary material.

Acknowledgments

This work was supported by the US National Institutes of Health grants R00EB013450 (S.L) and the US Department of Defense grants, CA130460 (S.L., Y.O.) and PC131920 (M.S). This work also supported in part by the National Research Foundation of Korea grants, Global Research Laboratory Program NRF-2013K1A1A2002050115 (M.G.P., S.L., K.K. J.H.P), NRF-2013R1A1A2062043 (K.C.L.) and NRF-2013R1A1A2064165 (S.M.L.).

References

1. Ashkenazi A, Herbst RS. To kill a tumor cell: the potential of proapoptotic receptor agonists. J Clin Invest. 2008; 118:1979–1990. [PubMed: 18523647]
2. Johnstone RW, Frew AJ, Smyth MJ. The TRAIL apoptotic pathway in cancer onset, progression and therapy. Nat Rev Cancer. 2008; 8:782–798. [PubMed: 18813321]
3. Allen JE, El-Deiry WS. Regulation of the human TRAIL gene. Cancer Biol Ther. 2012; 13:1143–1151. [PubMed: 22892844]
4. Ashkenazi A, Pai RC, Fong S, Leung S, Lawrence DA, Marsters SA, Blackie C, Chang L, McMurtrey AE, Hebert A, DeForge L, Koumenis IL, Lewis D, Harris L, Bussiere J, Koeppen H, Shahrokh Z, Schwall RH. Safety and antitumor activity of recombinant soluble Apo2 ligand. J Clin Invest. 1999; 104:155–162. [PubMed: 10411544]

5. Walczak H, Miller RE, Ariail K, Gliniak B, Griffith TS, Kubin M, Chin W, Jones J, Woodward A, Le T, Smith C, Smolak P, Goodwin RG, Rauch CT, Schuh JC, Lynch DH. Tumoricidal activity of tumor necrosis factor-related apoptosis-inducing ligand in vivo. Nature Med. 1999; 5:157–163. [PubMed: 9930862]

6. Stuckey DW, Shah K. TRAIL on trial: preclinical advances in cancer therapy. Trends Mol Med. 2013; 19:685–694. [PubMed: 24076237]

7. Herbst RS, Eckhardt SG, Kurzrock R, Ebbinghaus S, O'Dwyer PJ, Gordon MS, Novotny W, Goldwasser MA, Tohnya TM, Lum BL, Ashkenazi A, Jubb AM, Mendelson DS. Phase I dose-escalation study of recombinant human Apo2L/TRAIL, a dual proapoptotic receptor agonist, in patients with advanced cancer. J Clin Oncol. 2010; 28:2839–2846. [PubMed: 20458040]

8. Leong S, Cohen RB, Gustafson DL, Langer CJ, Camidge DR, Padavic K, Gore L, Smith M, Chow LQ, von Mehren M, O'Bryant C, Hariharan S, Diab S, Fox NL, Miceli R, Eckhardt SG. Mapatumumab, an antibody targeting TRAIL-R1, in combination with paclitaxel and carboplatin in patients with advanced solid malignancies: results of a phase I and pharmacokinetic study. J Clin Oncol. 2009; 27:4413–4421. [PubMed: 19652058]

9. Soria JC, Mark Z, Zatloukal P, Szima B, Albert I, Juhasz E, Pujol JL, Kozielski J, Baker N, Smethurst D, Hei YJ, Ashkenazi A, Stern H, Amler L, Pan Y, Blackhall F. Randomized phase II study of dulanermin in combination with paclitaxel, carboplatin, and bevacizumab in advanced non-small-cell lung cancer. J Clin Oncol. 2011; 29:4442–4451. [PubMed: 22010015]

10. Trarbach T, Moehler M, Heinemann V, Kohne CH, Przyborek M, Schulz C, Sneller V, Gallant G, Kanzler S. Phase II trial of mapatumumab, a fully human agonistic monoclonal antibody that targets and activates the tumour necrosis factor apoptosis-inducing ligand receptor-1 (TRAIL-R1), in patients with refractory colorectal cancer. Br J Cancer. 2010; 102:506–512. [PubMed: 20068564]

11. Dimberg LY, Anderson CK, Camidge R, Behbakht K, Thorburn A, Ford HL. On the TRAIL to successful cancer therapy? Predicting and counteracting resistance against TRAIL-based therapeutics. Oncogene. 2013; 32:1341–1350. [PubMed: 22580613]

12. Lemke J, von Karstedt S, Zinngrebe J, Walczak H. Getting TRAIL back on track for cancer therapy. Cell Death Differ. 2014; 21:1350–1364. [PubMed: 24948009]

13. Newsom-Davis T, Prieske S, Walczak H. Is TRAIL the holy grail of cancer therapy? Apoptosis. 2009; 14:607–623. [PubMed: 19194800]

14. Hellwig CT, Rehm M. TRAIL signaling and synergy mechanisms used in TRAIL-based combination therapies. Mol Cancer Ther. 2012; 11:3–13. [PubMed: 22234808]

15. Voelkel-Johnson C. TRAIL-mediated signaling in prostate, bladder and renal cancer. Nat Rev Urol. 2011; 8:417–427. [PubMed: 21670755]

16. Kelley SK, Harris LA, Xie D, Deforge L, Totpal K, Bussiere J, Fox JA. Preclinical studies to predict the disposition of Apo2L/tumor necrosis factor-related apoptosis-inducing ligand in humans: characterization of in vivo efficacy, pharmacokinetics, and safety. J Pharmacol Exp Ther. 2001; 299:31–38. [PubMed: 11561060]

17. Ashkenazi A, Holland P, Eckhardt SG. Ligand-based targeting of apoptosis in cancer: the potential of recombinant human apoptosis ligand 2/Tumor necrosis factor-related apoptosis-inducing ligand (rhApo2L/TRAIL). J Clin Oncol. 2008; 26:3621–3630. [PubMed: 18640940]

18. Harris JM, Chess RB. Effect of pegylation on pharmaceuticals. Nat Rev Drug Discov. 2003; 2:214–221. [PubMed: 12612647]

19. Ganten TM, Koschny R, Sykora J, Schulze-Bergkamen H, Buchler P, Haas TL, Schader MB, Untergasser A, Stremmel W, Walczak H. Preclinical differentiation between apparently safe and potentially hepatotoxic applications of TRAIL either alone or in combination with chemotherapeutic drugs. Clin Cancer Res. 2006; 12:2640–2646. [PubMed: 16638878]

20. Pasut G, Veronese FM. PEG conjugates in clinical development or use as anticancer agents: an overview. Adv Drug Deliv Rev. 2009; 61:1177–1188. [PubMed: 19671438]

21. Chae SY, Kim TH, Park K, Jin CH, Son S, Lee S, Youn YS, Kim K, Jo DG, Kwon IC, Chen X, Lee KC. Improved antitumor activity and tumor targeting of NH(2)-terminal-specific PEGylated tumor necrosis factor-related apoptosis-inducing ligand. Mol Cancer Ther. 2010; 9:1719–1729. [PubMed: 20515949]

22. Kim TH, Youn YS, Jiang HH, Lee S, Chen X, Lee KC. PEGylated TNF-related apoptosis-inducing ligand (TRAIL) analogues: pharmacokinetics and antitumor effects. Bioconjug Chem. 2011; 22:1631–1637. [PubMed: 21751817]

23. Drosopoulos KG, Roberts ML, Cermak L, Sasazuki T, Shirasawa S, Andera L, Pintzas A. Transformation by oncogenic RAS sensitizes human colon cells to TRAIL-induced apoptosis by up-regulating death receptor 4 and death receptor 5 through a MEK-dependent pathway. J Biol Chem. 2005; 280:22856–22867. [PubMed: 15757891]

24. Stolfi R, Caruso E, Franze A, Rizzo A, Rotondi I, Monteleone MC, Fantini F, Pallone G. Monteleone 2-methoxy-5-amino-N-hydroxybenzamide sensitizes colon cancer cells to TRAIL-induced apoptosis by regulating death receptor 5 and survivin expression. Mol Cancer Ther. 2011; 10:1969–1981. [PubMed: 21817114]

25. Lacour S, Micheau O, Hammann A, Drouineaud V, Tschopp J, Solary E, Dimanche-Boitrel MT. Chemotherapy enhances TNF-related apoptosis-inducing ligand DISC assembly in HT29 human colon cancer cells. Oncogene. 2003; 22:1807–1816. [PubMed: 12660816]

26. Vrielink J, Heins MS, Setroikromo R, Szegezdi E, Mullally MM, Samali A, Quax WJ. Synthetic constrained peptide selectively binds and antagonizes death receptor 5. FEBS J. 2010; 277:1653–1665. [PubMed: 20156289]

27. Muhlenbeck F, Haas E, Schwenzer R, Schubert G, Grell M, Smith C, Scheurich P, Wajant H. TRAIL/Apo2L activates c-Jun NH2-terminal kinase (JNK) via caspase-dependent and caspase-independent pathways. J Biol Chem. 1998; 273:33091–33098. [PubMed: 9830064]

28. Dolloff NG, Mayes PA, Hart LS, Dicker DT, Humphreys R, El-Deiry WS. Off-target lapatinib activity sensitizes colon cancer cells through TRAIL death receptor up-regulation. Sci Transl Med. 2011; 3:86ra50.

29. Fu L, Lin YD, Elrod HA, Yue P, Oh Y, Li B, Tao H, Chen GZ, Shin DM, Khuri FR, Sun SY. c-Jun NH2-terminal kinase-dependent upregulation of DR5 mediates cooperative induction of apoptosis by perifosine and TRAIL. Mol Cancer. 2010; 9:315. [PubMed: 21172010]

30. Bennett BL, Sasaki DT, Murray BW, O'Leary EC, Sakata ST, Xu W, Leisten JC, Motiwala A, Pierce S, Satoh Y, Bhagwat SS, Manning AM, Anderson DW. SP600125, an anthrapyrazolone inhibitor of Jun N-terminal kinase. Proc Natl Acad Sci U S A. 2001; 98:13681–13686. [PubMed: 11717429]

31. Choi KY, Jeon EJ, Yoon HY, Lee BS, Na JH, Min KH, Kim SY, Myung SJ, Lee S, Chen X, Kwon IC, Choi K, Jeong SY, Kim K, Park JH. Theranostic nanoparticles based on PEGylated hyaluronic acid for the diagnosis, therapy and monitoring of colon cancer. Biomaterials. 2012; 33:6186–6193. [PubMed: 22687759]

32. Choi KY, Chung H, Min KH, Yoon HY, Kim K, Park JH, Kwon IC, Jeong SY. Self-assembled hyaluronic acid nanoparticles for active tumor targeting. Biomaterials. 2010; 31:106–114. [PubMed: 19783037]

33. Choi KY, Yoon HY, Kim JH, Bae SM, Park RW, Kang YM, Kim IS, Kwon IC, Choi K, Jeong SY, Kim K, Park JH. Smart nanocarrier based on PEGylated hyaluronic acid for cancer therapy. ACS Nano. 2011; 5:8591–8599. [PubMed: 21967065]

34. Choi KY, Saravanakumar G, Park JH, Park K. Hyaluronic acid-based nanocarriers for intracellular targeting: interfacial interactions with proteins in cancer. Colloids Surf B Biointerfaces. 2012; 99:82–94. [PubMed: 22079699]

35. Swierczewska M, Choi KY, Mertz EL, Huang X, Zhang F, Zhu L, Yoon HY, Park JH, Bhirde A, Lee S, Chen X. A facile, one-step nanocarbon functionalization for biomedical applications. Nano Lett. 2012; 12:3613–3620. [PubMed: 22694219]

36. Liu G, Choi KY, Bhirde A, Swierczewska M, Yin J, Lee SW, Park JH, Hong JI, Xie J, Niu G, Kiesewetter DO, Lee S, Chen X. Sticky nanoparticles: a platform for siRNA delivery by a bis(zinc(II) dipicolylamine)-functionalized, self-assembled nanoconjugate. Angew Chem Int Ed Engl. 2012; 51:445–449. [PubMed: 22110006]

37. Yoon HY, Kim HR, Saravanakumar G, Heo R, Chae SY, Um W, Kim K, Kwon IC, Lee JY, Lee DS, Park JC, Park JH. Bioreducible hyaluronic acid conjugates as siRNA carrier for tumor targeting. J Control Release. 2013; 172:653–661. [PubMed: 24055507]

38. Rahman A, Carmichael D, Harris M, Roh JK. Comparative pharmacokinetics of free doxorubicin and doxorubicin entrapped in cardiolipin liposomes. Cancer Res. 1986; 46:2295–2299. [PubMed: 3697976]

39. Jiang J, Liu X, Deng L, Zhang P, Wang G, Wang S, Liu H, Su Y. GMP production and characterization of leucine zipper-tagged tumor necrosis factor-related apoptosis-inducing ligand (LZ-TRAIL) for phase I clinical trial. Eur J Pharmacol. 2014; 740:722–732. [PubMed: 24929054]

40. Maeda H, Nakamura H, Fang J. The EPR effect for macromolecular drug delivery to solid tumors: Improvement of tumor uptake, lowering of systemic toxicity, and distinct tumor imaging in vivo. Adv Drug Deliv Rev. 2013; 65:71–79. [PubMed: 23088862]

41. Ghosh SC, Alpay S Neslihan, Klostergaard J. CD44: a validated target for improved delivery of cancer therapeutics. Expert Opin Ther Targets. 2012; 16:635–650. [PubMed: 22621669]

42. Hrkach J, Hoff D Von, Mukkaram Ali M, Andrianova E, Auer J, Campbell T, Witt D De, Figa M, Figueiredo M, Horhota A, Low S, McDonnell K, Peeke E, Retnarajan B, Sabnis A, Schnipper E, Song JJ, Song YH, Summa J, Tompsett D, Troiano G, Van Geen Hoven T, Wright J, LoRusso P, Kantoff PW, Bander NH, Sweeney C, Farokhzad OC, Langer R, Zale S. Preclinical development and clinical translation of a PSMA-targeted docetaxel nanoparticle with a differentiated pharmacological profile. Sci Transl Med. 2012; 4:128ra139.

43. Schutz CA, Juillerat-Jeanneret L, Mueller H, Lynch I, Riediker M. Therapeutic nanoparticles in clinics and under clinical evaluation. Nanomedicine (Lond). 2013; 8:449–467. [PubMed: 23477336]

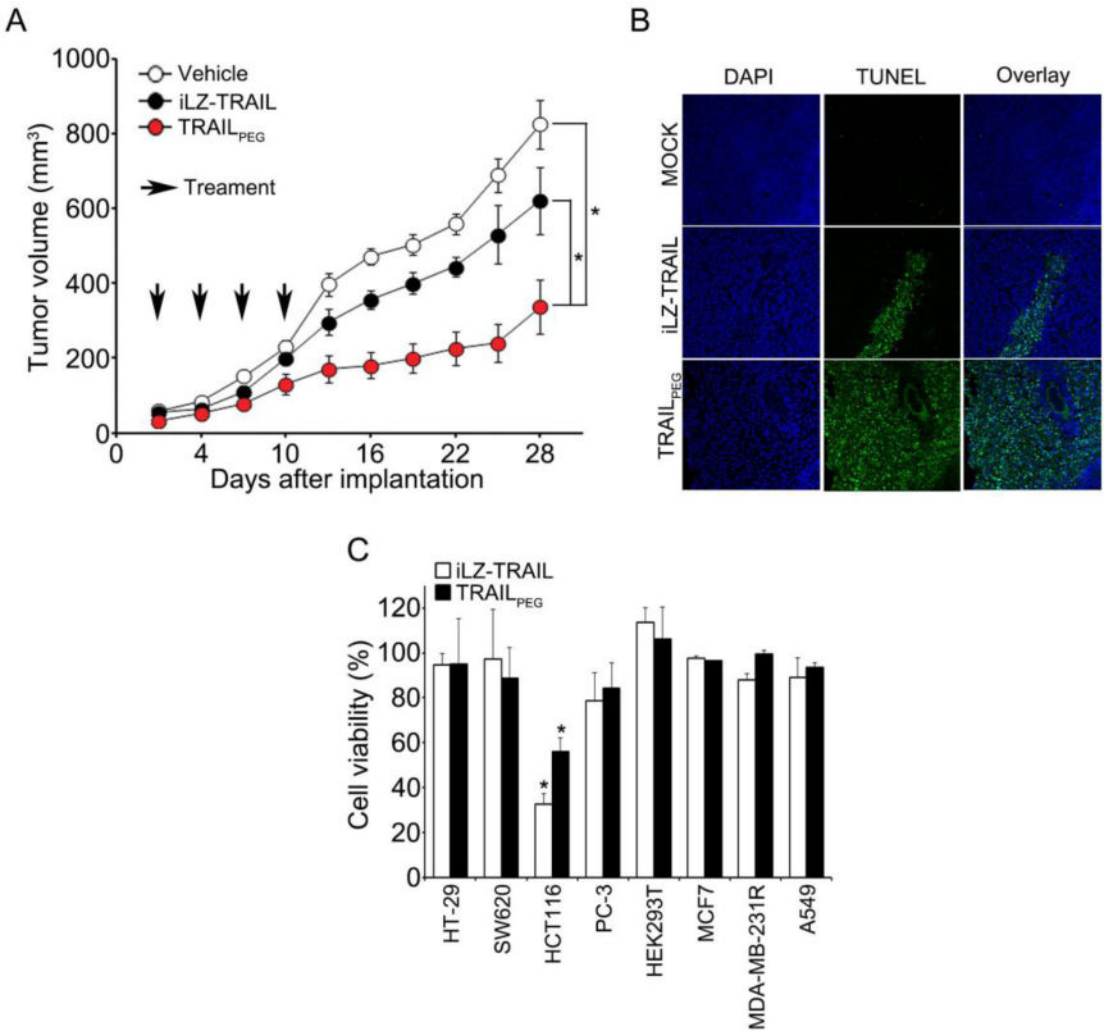

Figure 1.

TRAIL$_{PEG}$ has superior tumor growth inhibition effects over non-PEGylated TRAIL in TRAIL-sensitive xenografts, despite having a lower potency in vitro. (A) HCT116 xenografts were established and mice were intravenously treated when the tumor was palpable with four rounds of saline, iLZ-TRAIL (200 μg) or TRAIL$_{PEG}$ (200 μg, protein-based). Tumor volumes were determined by caliper measurements (n=5/group). Values indicate means ± SEM. (B) TUNEL staining of harvested tumors after control (mock), iLZ-TRAIL or TRAIL$_{PEG}$ treatment from (A). Fluorescence images were acquired under a confocal microscope and overlaid with Hoechst 33258 staining. (C) Human tumor cell lines: colon (HT-29, SW620, HCT116), prostate (PC3), breast (MDA-MB-231R, MCF7) and lung (A549) and normal human cell line: kidney (HEK293T) were collected and examined for their sensitivities to iLZ-TRAIL and TRAIL$_{PEG}$ by cell viability assay. Cells were treated with TRAIL variants (1 μg/mL, protein-based) for 24 h and cell death rates were measured by MTT assay (n = 3). Values indicate means ± SD. $^{*}P$ <0.001 vs. control group (without any treatment).

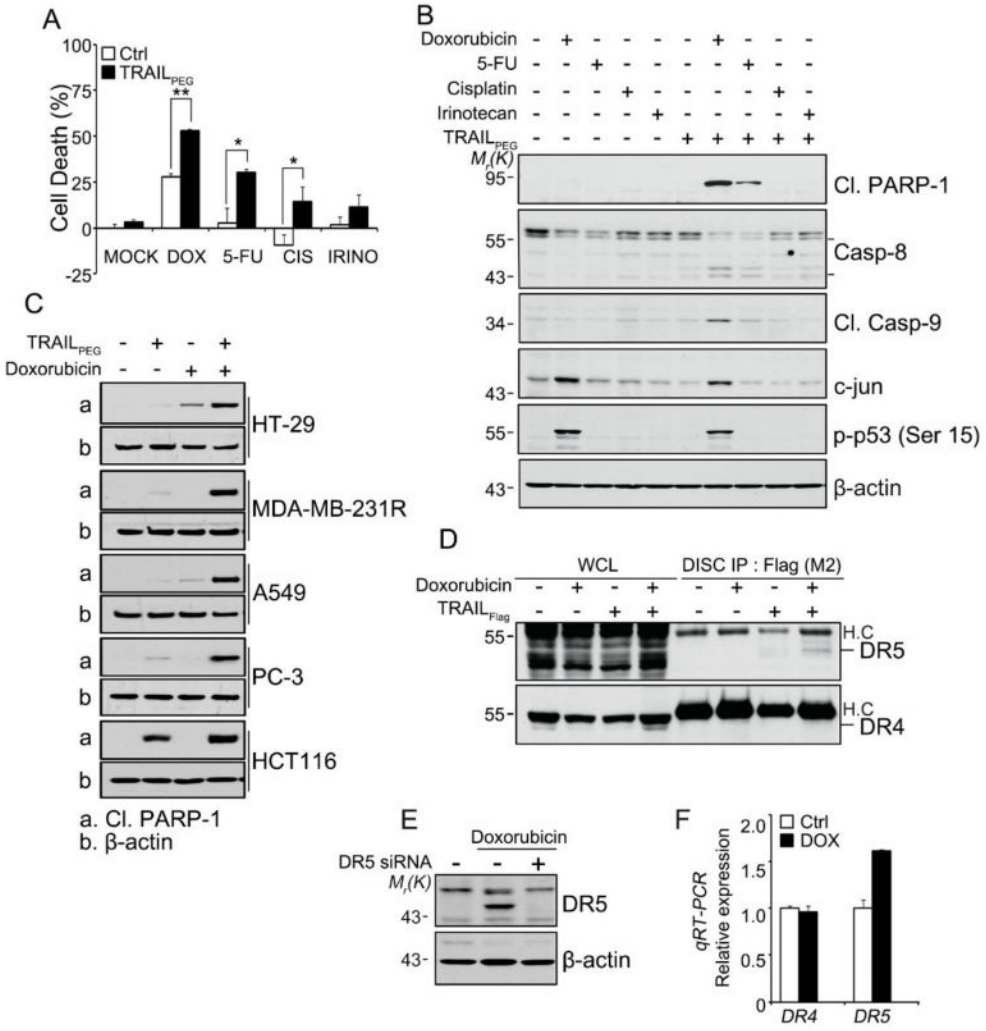

Figure 2.

Doxorubicin (DOX) induces apoptosis when combined with $TRAIL_{PEG}$ in TRAIL-resistant cancer cell lines. (A) DNA damaging agents sensitize TRAIL-resistant HT-29 cells to cell death after $TRAIL_{PEG}$ treatment. HT-29 cells were treated with sublethal doses of doxorubicin (DOX, 2 μg/mL), 5-fluorouracil (5-FU, 10 μg/mL), cisplatin (CIS, 2 μg/mL) and irinotecan (IRINO, 2.9 μg/mL) for 24 h and further incubated with $TRAIL_{PEG}$ (1 μg/mL) for an additional 24 h. The cell death rates were measured by MTT assay (n = 3). *$P < 0.001$ vs. cells treated with cytotoxic agent only (Ctrl). Values indicate means ± SD. (B) The cell extracts were prepared and the levels of apoptosis-related proteins were examined by western blotting; cleaved PARP-1 (Cl. PARP-1), caspase-8 (Casp-8), cleaved Casp-8, c-Jun and phospho-p53 (p-p53). β-actin was used as a protein loading control. (C) A combination of $TRAIL_{PEG}$ and DOX but not drug alone sensitizes TRAIL-induced apoptosis as seen by cleaved PARP-1, a hallmark of apoptosis, in various TRAIL-resistant cells, HT-29 (colon), MDA-MB-231 (breast), A549 (lung), and PC3 (prostate), as in TRAIL-sensitive HCT116 (colon) cancer cells. (D) DISC formation in HT-29 cells. HT-29 cells were left untreated or stimulated with 500 ng/ml of $TRAIL_{Flag}$ for 1 h. The lysates were immunoprecipitated with FLAG (M2) and analyzed by Western blotting using DR4

and DR5 antibodies. WCL: Whole cell lysates. (E and F) DR5 induction in HT-29 cells by DOX. (E) HT-29 cells were transfected with DR5 siRNA for 48 h and the cells were left untreated or incubated with DOX for an additional 24 h. Cell extracts were examined by western blotting for DR5 using anti-DR5 and anti-β-actin antibodies. β-actin was used as a protein loading control. (F) HT-29 cells were treated with DOX for 24 h and the cell extracts were examined for mRNA levels of DR4 and DR5 using gene-specific primers by qRT-PCR analysis.

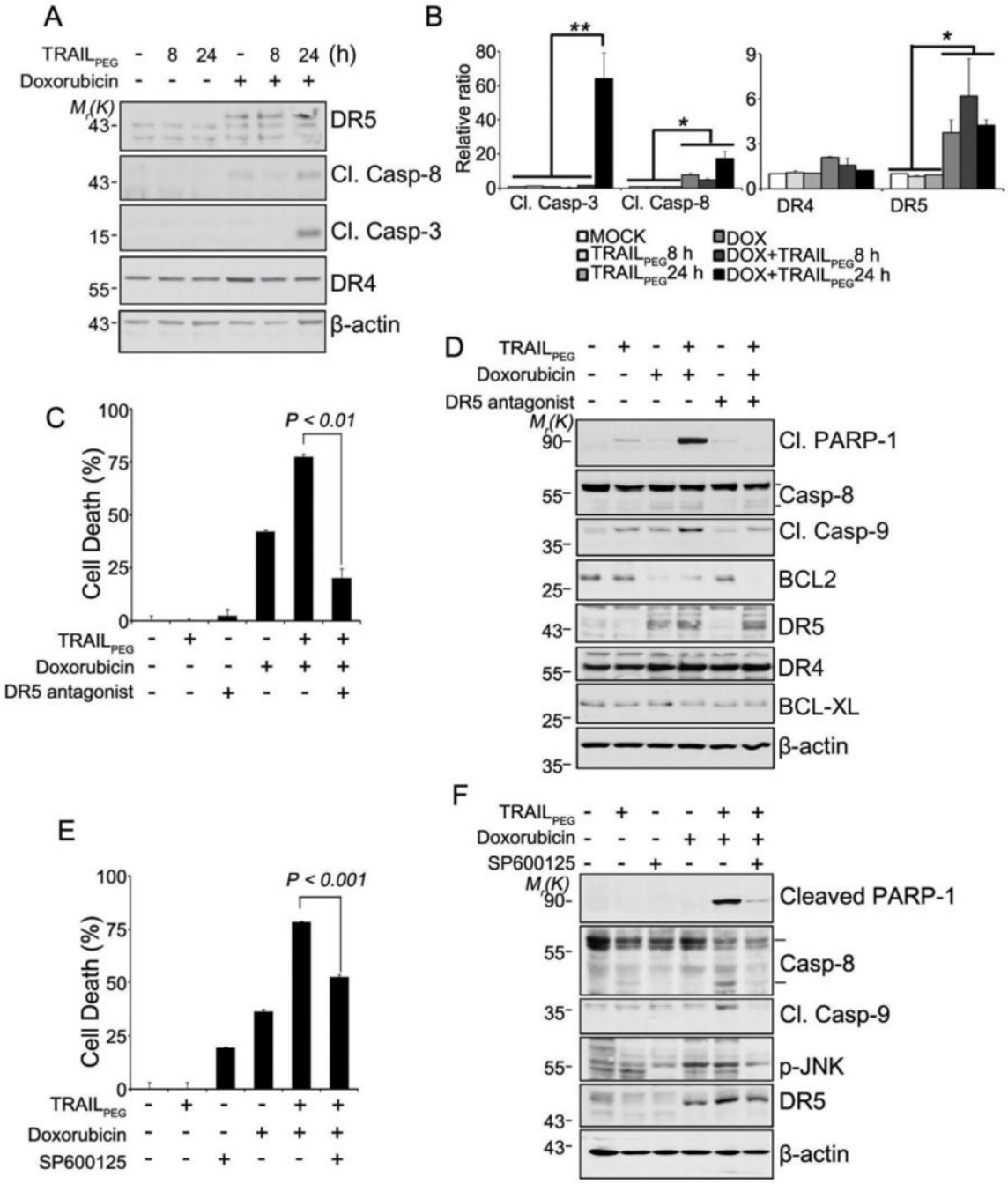

Figure 3.

When combined with $TRAIL_{PEG}$, DOX synergizes TRAIL-induced apoptosis in HT-29 cells through DR5 upregulation and partially by JNK-mediated apoptosis. (A) Western blotting analysis of HT-29 cells treated with $TRAIL_{PEG}$ (1 μg/mL) and DOX (2 μg/mL) alone or in combination with different incubation times. The cell extracts were prepared and the levels of DR4, DR5 and cleaved caspase-8 (Cl. Casp-8) and caspase-3 (Cl. Casp-3) were examined. (B) The relative fold increase of cleaved caspase-3, caspase-8, DR4 and DR5 expressions from control group (no $TRAIL_{PEG}$ (1 μg/mL) and DOX (2 μg/mL) treatment).

*$P < 0.05$, **$P < 0.001$ vs. groups (C) The effect of upregulated DR5 on TRAIL-induced cell death in HT-29 cells. Cells were treated with DOX (2 μg/mL) and $TRAIL_{PEG}$ (1 μg/mL) alone or in combination with or without DR5-A (2 μg/mL, DR5 antagonist peptide) pretreatment. Cell death rates were measured by MTT assay (n = 3). *$P < 0.001$ vs. DR5 neutralized group. (D) Western blotting analysis of cells as treated in (C). Cleaved caspases, PARP-1, DR4 and DR5, BCL2, BCL-XL and β-actin (loading control) was measured. (E) The effect of JNK on TRAIL-induced cell death in HT-29 cells. Cells were treated with DOX (2 μg/mL) and $TRAIL_{PEG}$ (1 μg/mL) alone or in combination with or without SP600125 (JNK inhibitor, 20 μM) pre-treatment. Cell death rates were measured by MTT assay (n = 3). *$P < 0.001$ vs. JNK activity inhibited group. (F) Cleaved caspases, PARP-1, phosphorylated JNK and DR5 western blot analysis of cells in (E). β-actin was measured as a loading control.

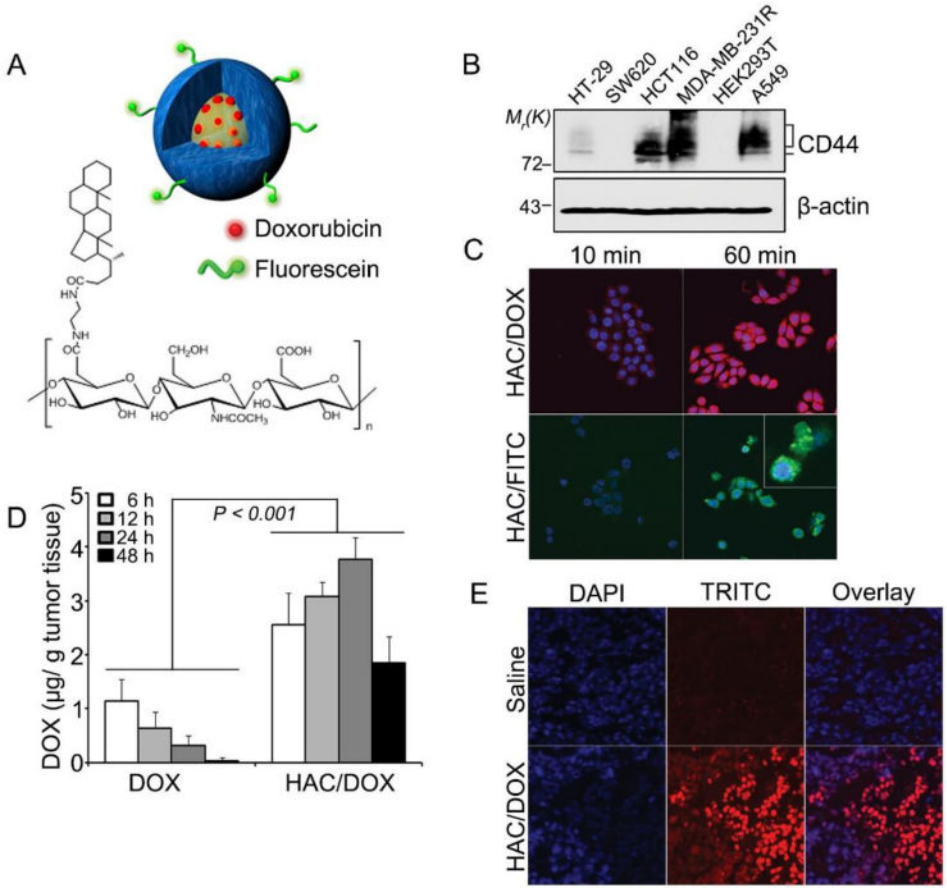

Figure 4.

HAC/DOX but not free DOX accumulates in tumors for a sustained period of time and potentiates caspase cascade when combined with $TRAIL_{PEG}$. (A) Upper; schematic diagram of HAC/DOX, hyaluronic acid-based conjugate (HAC) carrying doxorubicin in the core and FITC dye molecules labeled on the surface for fluorescence microscopy. Lower; a chemical structure of HAC, hyaluronic acid chemically conjugated with cholanic acid. (B) Cancer cells were examined for their CD44 expression. The cell extracts were prepared and the levels of CD44 were examined by western blotting. (C) HAC/DOX rapidly internalizes and releases DOX in HT-29 cells. HT-29 cells were incubated with HAC/DOX (2 μg/mL, doxorubicin-based) for 10 min and 60 min. Fluorescence images were acquired under a confocal microscope and overlaid with DAPI staining. Representative images are based on four different measurements. HAC; green (FITC, ex/em: 490/525), DOX; red (TRITC, ex/em: 557/576), and nucleus; blue (DAPI, ex/em: 350/470). FACS analysis described in Supplementary Fig. S4. (D) DOX concentration in the harvested tumors following single intravenous dosing of DOX (7 mg/kg) and HAC/DOX (7 mg/kg, DOX-based) in HT-29 xenografts. When tumors reached a diameter of 300 mm^3, mice were intravenously treated with DOX and HAC/DOX. At the indicated time points, mice were sacrificed and the tumor concentration of doxorubicin were measured by a fluorescence absorbance method followed by extraction recovery (n = 3). Values indicate means ± S.D. (E) The uptake and distribution of doxorubicin in tumor tissues. Representative fluorescence images of tumor sections

demonstrate the high accumulation of doxorubicin after HAC/DOX injection. Nucleus; blue (DAPI ex/em: 350/470), doxorubicin; red (TRITC; ex/em: 557/576).

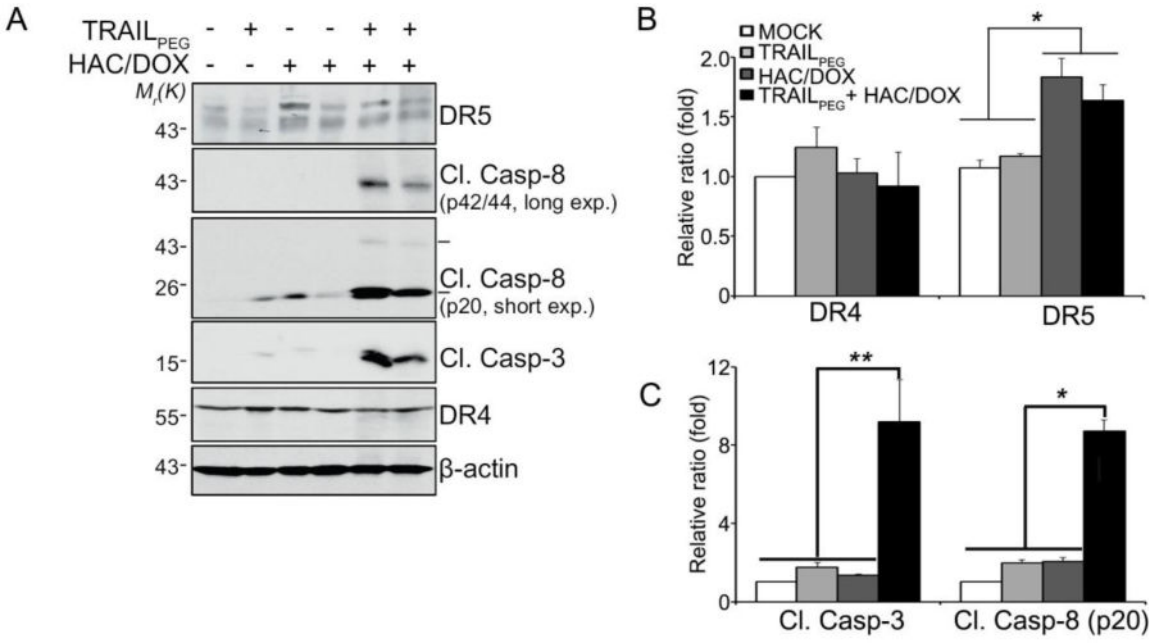

Figure 5.

Simultaneous treatment of $TRAIL_{PEG}$ and HAC/DOX initiates apoptosis in TRAIL-resistant tumors in vivo. (A) Lysates of HT-29 tumors from mice treated with $TRAIL_{PEG}$ (200 μg per mouse) and HAC/DOX (7 mg/kg, DOX-based) alone or in combination were western blotted for death receptors (DR5, DR4), cleaved caspases and β-actin (loading control) expression analysis. Two representative western blot analyses are shown for each $TRAIL_{PEG}$ group. (B, C) The relative fold increase of DR and caspase expressions $*P < 0.05$, $**P < 0.001$ vs. groups.

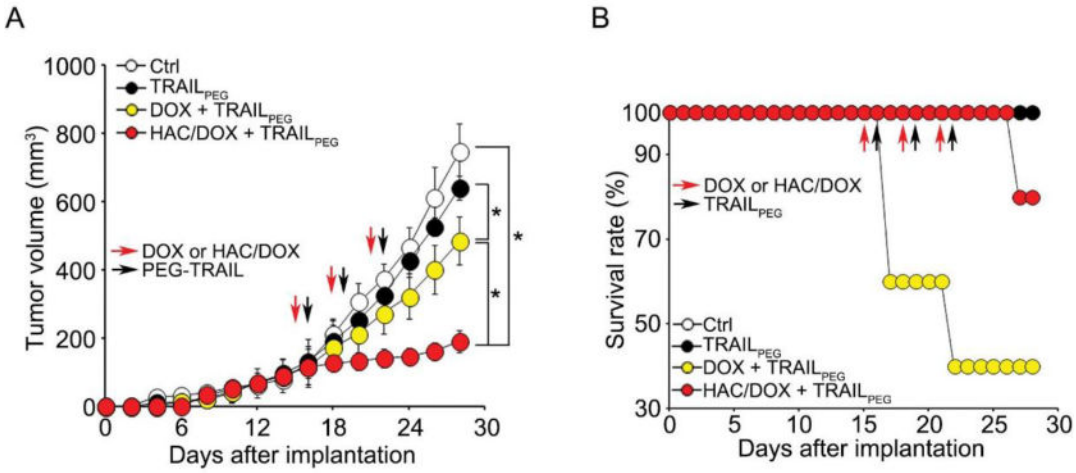

Figure 6.

Simultaneous treatment of $TRAIL_{PEG}$ and HAC/DOX reduces tumor growth in TRAIL-resistant tumors and reduces toxicity by DOX in vivo. (A) Mice bearing approximately 150 mm^3 HT-29 tumors were intravenously treated with vehicle, $TRAIL_{PEG}$ (200 μg) alone, $TRAIL_{PEG}$ (200 μg) combined with DOX (7 mg/kg) or HAC/DOX (7 mg/kg, DOX-based) every 3 days starting at day 15 for a total of 3 doses. Tumor volumes were determined by caliper measurements (n=5/group).Values indicate means ± SEM. (B) Survival rate curve of mice treated in (A).